UNIVERSITY OF HELSINKI

A methodological comparison of bathymetric modelling in large sub-arctic rivers – case study in Tana River, Finland

Possible subtitle

Master's Programme in Geography, Geoinformatics
Master's thesis

Author:
Susanna Kukkavuori

Supervisor(s):
PhD Petteri Muukkonen
PhD Tua Nylén

x.x.202x
Helsinki

Faculty: Faculty of Science
Degree programme: Master's Programme in Geography
Study track: Geoinformatics
Author: Susanna Kukkavuori
Title: A methodological comparison of bathymetric modelling in large sub-arctic rivers – case study in Tana River, Finland
Level: Master's thesis
Month and year: xx.202x
Number of pages: xx
Keywords: multibeam sonar, laser scanning, satellite imagery, bathymetric mapping, sub-arctic river
Supervisor or supervisors: Petteri Muukkonen (PhD), Tua Nylén (PhD)
Where deposited: University of Helsinki electronic theses library E-thesis/HELDA
Additional information:
Abstract:

Table of contents

1 Introduction

Haven’t modified this chapter a lot since spring

Efficient, accurate and cost-effective methods to model river bathymetry are a common good and great benefit amongst earth scientists (Kinzel et al., 2013). Detailed information of river bathymetry may assist with questions related to for example hydrology related management and decision-making issues, sustainable development, future conditions and how to prepare for them. For to understand and gain knowledge of many essential hydrological and environmental factors on riverine environments, for example stream velocity, sediment transportation and littoral habitat mapping to name a few, it is beneficial to know every physical aspect of underwater morphology and topography (Flener et al., 2012). In the Arctic region, the climate change has warmed the area more than six time the global average in the last decade (Huang et al., 2017), which is affecting for example the local environments, landscapes habitats, livelihoods, species dramatically. Tana river being a large sub-arctic river, it can provide essential information and future scenarios on river conditions in these changing temperatures.

In recent years shallow water monitoring techniques, and especially in river environments, have developed greatly (Alho et al., 2011; Kinzel et al., 2007). Especially active remote sensing techniques, e.g. airborne laser, allows shallow water modelling with high spatial and temporal resolution accuracy, and gains access to remote or otherwise hard-to-reach places. Traditionally, bathymetric models have been implemented from using field measurements and passive remote sensing methods, e.g. aerial imagery and echo-sounding, but have their limitations. For analysis to have an efficient workflow, it would be advisable to know what remote sensing method would compose most accurate model of river bathymetry and would be suitable to which fluvial condition.

Tana river morphology consist of fluvioglacial material, older fluviatile and glacio-marine sediments. At the lower course of the river, the sediments consists mostly of sand, silt and clay, and is quite erodible (Collinson, 1970; Mansikkaniemi, 1970). The main factors controlling the erosion and other modifications in the riverbed are wind, waves and changing currents. The magnitude of those impacts depends on local morphology, slope and on the duration and strength of the wind (Collinson, 1970).

Amongst other things, these geophysical elements are to be taken into consideration when trying to model the river bottom with most suitable remote sensing technique. The valley depth vary from 80 meters up to 300 meters deep (Mansikkaniemi, 1970), but that doesn't mean the average depth of the Tana river itself.

For the models to be useful in future studies, a proper assessment is in place. ~~So, the research questions for my thesis are: how accurately can different remote sensing methods model sub-arctic river bathymetry – what are their strengths and weaknesses, and are they affected by physical conditions of the river, and how.~~ Tana River is one of the sites being studied in research projects that aims to provide a dense, highly instrumented sites for freshwater monitoring. These research projects are Hydro-RDI Network, Hydro-RI Platform, and Green Digi-Basin that are project managed by Freshwater Competence Centre. This thesis is being done as a cooperation with FCC.

A methodological comparison of bathymetric modelling of sub-arctic river was conducted to evaluate the performance of different methods of bathymetric mapping. The study compared three methods: multibeam, lidar and satellite imagery.

This is not studied so much -> why? One reason can be that majority of the researches do not reach or do not live in cold areas/sub-arctic/arctic areas, and in addition in cold times (winter) those places can be hard to reach. In Canada there are larger rivers, so from there is couple of studies, but for now it is quite sparse (Lotsari, 2023).

Further research is indeed needed in this field of study. In addition to reasons above, combining field measurements, modelling and laboratory experiments can help improve our knowledge, planning and monitoring on river environmental changes in the midst of emerging global warming and its impacts on northern hemisphere. Astonishingly, the interlinking processes of ecosystems, sediment transport and yet signature character in the north, ice cover, are still far too little studied. Methodological studies and developments are much needed to understand these processes in ever changing conditions.

For the models to be useful in future studies, a proper assessment is in place. So, the research questions for the thesis are:

1) Is there a difference between remote sensing methods, how they perform on providing information on river bottom depth and topography? (workflow, filtering/clean-up/pre-processing, output)

2) Is there significant strengths and weaknesses in the methods based on modelled results? (outliers, no-data, performance in certain environment)

3) Does the modelling impact the accuracy of truthful topography information? (quantitative analysis part)

4) Do geomorphological and hydrological factors impact the accuracy of the models? (upstream vs downstream, rapids, sand/coarse material)

2 Background

2.1 River bottom topography

Originally, term ‘topography’ was related to place-description and in surveying and mapping the art of portraying details and paid little attention to observations on surface configuration. As the acknowledgement of the importance of surface expression in geology raised, the term was applied and in fact stated as a base to geology by geologist Clarence King (1842–1901), the director of the United States Geological Survey (USGS) somewhere around 1884: “the most fundamental connection of geology is with topography, because geology has for its purpose, either directly or remotely, the explanation of topography” (Johnson, 1887, p. 153).

Rapidly the relation of topography and environmental phenomena was recognised, for example in meteorology and characterising types of form both erosion and deposition, in land and under water (Johnson, 1887).

Tectonic processes, like plate movements, volcano eruptions and earthquakes, glaciers, climate and weather together with hydrology mold the base of Earth’s topography, causing deposition and erosion of material. From these dynamic factors the most powerful geomorphic factor is flowing water, reshaping the landscape constantly (Arbogast, 2017), naturally or by the actions of humans.

In erosion, materials, like rocks, sediments and soil, move from one place to another by geomorphic processes, to which stream flow is one of. Areas with high relief tend to influence stronger erosion and deposition effects due to help from forces gravity creates. Other factors creating erosion are climate and vegetation. Areas with dense vegetation are affected to erosion less than bare sites, as the vegetation protects sediment from erosion effectively. Climate causes rain, wind, drying, freezing etc. that cause erosion. The more extreme weather, more intense erosion (Arbogast, 2017). The deposition of material acts as a opposite to erosion. Deposition occurs, when material transporting factor stops or loses its powers to move material. Deposition of eroded material tends to take place at the base, where slope gently descents and the effect of gravity lessens.

Flowing water starts to erode hills and slopes by rills, from which they coalesce and enlarge, forming gullies and even board canyons. The geometrical attributes, so called hydraulic geometry of river channels can be defined with following variables:

A) channel width (w), that is how wide the channel basin is where the water flows

B) depth (d), that is the depth of the channel from the surface of water to the channel bed

C) velocity (v), that is how rapid the water flows in the channel. From where velocity is measured, the value varies: at the sides and bottom of channel, velocity is slower due to frictional forces. Flow velocity is fastest in the middle of a channel

D) slope (s), that is how big slope or sometimes called gradient is where the water flows

E) discharge (Q), that is how much water there flows in a channel.

The size of the channel can be calculated for example by how much water flows through it by this following simple equation:

$$Q = w * d * v \quad (1).$$

Hydraulic variables are interrelated to one another, meaning that every variable changes the others value (Arbogast, 2017).

Together with river channel topography formation and erosion and deposition caused by geomorphic forces shapes the topography of the channel itself but also the bed of channel (Legleiter, 2012).

Modelling the topography of river bottom with GIS acts an important role when studying environment's hydrological processes. For example, forecasting flood catchment areas and urban stormwater (e.g. Beven & Kirkby (1979) and Djokic & Maidment (1991)), predicting flow depth, velocity, spatial flow paths and networks

(e.g. Quinn et al. (1991)), as well as modelling water quality and soil erosion (e.g. Vieux (1991) and Wright & Webster (1991)). Topographic models of river bottom can be applied to non-hydrological research applications also (Milne & Sear, 1997), for example modelling landslides, soil-landscape, landform mapping and rainfall (e.g. Carrara et al. (1991), Gessler et al. (1995), Hutchinson & Dowling (1991) and Tribe (1992)).

How well is river bottoms known aka modelled/studied -> in focus region and in general

- pohjoisten jokien pohjanmuodoissa, prosesseissa, tutkimustiedossa tai olemassa olevassa datassa jotain sellaista erityistä, minkä takia on tarpeen tutkia syvyysdataa juuri näillä alueilla?
- Joko tässä kappaleessa tai sitten uudessa kappaleessa voisi vielä kuvata uudehkoja menetelmiä ja niiden uusia sovelluskohteita. Eli selittää, että kaukokartoitusala kehittyy nopeasti ja tuo uusia menetelmiä syvyyskartoitukseen. Niiden testaaminen eri tyyppisissä ympäristöissä on vielä alkutekijöissään, joten tämä tutkimus ja opinnäytetyö on kontribuutio alalle.

New methods, approaches, applications, models, and testing them in different sub-arctic and artic river environment are much needed to understand the impacts warming weather might cause to river processes, but much of it are still lacking.

- Previous studies tulee tähän kohtaan luontevasti

What has been studied before relating to the subject, are related to sediment transportation and river ice-coverage, that might cause river erosion [CITE]. Much of the work has been conducted from northern countries, for example here in Finland, and in Canada, where there are large rivers and long cold season periods [CITE].

Comparison of remote sensing methods ability to map bathymetry on river have conducted for example Kasvi et al. (2019) studying efficiency of echo sounding and photogrammetry in clear, shallow river in subarctic Finland, as Shintani & Fonstad (2017) in their research studying the abilities of photogrammetry and spectral depth approaches in a gravel-bed river in Oregon, United States, and Woodget et al. (2015) quantifying the performance of photogrammetry and LiDAR.

2.2 Large sub-arctic rivers

There is no one connotation to describe the term “sub-arctic”, but how it is usually comprehended, it covers the area where boreal forest phytogeographical region starts in Northern Hemisphere (Hare, 1951). For biodiversity, sub-arctic river valleys are hotspots because of their varying geodiversity (Nylén et al., 2019). In sub-arctic regions there is usually variation in geology, topography and in the processes of earth surface, for example post-glacial rebound (SITE). Together these processes transport material – organic and inorganic – providing habitats and microhabitats for species above and under water (e.g. Gould & Walker (1999)), and providing local communities, mostly native Sámi, a livelihood, in forms of for example fishery (Alioravainen et al., 2023) and tourism.

The importance of ice cover and the effects of it in sub-arctic and arctic regions have only recently emerged (Turcotte et al., 2011). The research field lacks on detailed field data and descriptions on how river ice impacts channel erosion, transports fine sediment and gravels, and other data from different settings, for example climatic and hydrological, in addition to morphological impacts (Lotsari et al., 2015, 2020; Turcotte et al., 2011). Even scarcer amount of studies are utilizing remote sensing methods to gather that data for that matter (Lotsari et al., 2015). With remote sensing methods, for example laser scanning, far more accurate data with adequate resolution, from wider spatial range and remote locations that can be hard-to-reach could be acquired less time consumingly and more often. Multitemporal data would reveal vital knowledge of how factors mentioned above could impact river dynamics in long run.

Snow and ice covers the land and waters on sub-arctic regions almost half a year or longer (Bennett et al., 2022), and hence has major impact on region’s environment and ecosystem. A characteristic phenomenon to sub-arctic region, and important event for hydrologic cycle is floods in spring, when snow cover starts to melt (Ford & Bedford, 1987). Snowpack accumulation during winter determines the magnitude of spring discharge. Other factors processes impacting flood magnitude are precipitation, evaporation, temperature and runoff from basin, alongside with region topography (Dahlke et al., 2012). Floods can export sediment loads in various size depending on their magnitude and cause changes in surrounding environment.

Sub-arctic region is facing crucial times and perhaps already crossed the tipping point. Global warming mainly due to climate change causes shifts in ecosystems as in landscapes in Northern Hemisphere maybe now more than ever (Huang et al., 2017; Magnuson et al., 2000; Weyhenmeyer et al., 2011). Multiple studies from recent years have shown how sub-arctic and especially arctic region has warmed nearly four times faster than global average in last decades (Rantanen et al., 2022). Warming appears especially as shorter periods in snow coverage and river (and lake and sea) ice formations, and in increasing of precipitation in forms of water. These are consequences from multiple causes, for example shifts in ocean currents (e.g. Smeed et al. (2018)), and air pollution (e.g. Ruppel et al. (2021)). For predicting consequences for sub-arctic river ecosystems these climate change impacts causes, it is vital to have accurate, multitemporal and continuous monitoring, data gathering and analysis of those regions. For that, further studies for implementing adequate methods to achieve that is necessary.

2.3 Interaction of electromagnetic radiation with atmosphere, water and sediment

Environmental factors influence the remote sensed radiation (Curran & Novo, 1988). For convenience they are grouped to those that relates to atmosphere, the boundary between atmosphere and water, water column and depth, and sediment.

2.3.1 Atmosphere

Atmosphere can affect the amount and quality of electromagnetic radiation from target to sensor. Different gases, particles and pressures causes different radiation absorption, scattering and transmission, that affects how electromagnetic radiation is received and detected in remote sensing sensors. Factors in the atmosphere are divided into two groups after Bowker et al. (1985) based on their characteristics: meteorological parameters and optical parameters. Meteorological parameters include relative humidity, cloud cover and surface pressure, whereas atmospheric optical parameters include visual range (V), aerosol type and single-scattering albedo (ω_0). Optical parameters are also addressed as optical thickness (Bowker et al., 1985).

Humidity, temperature and pressure can influence the index of refraction of air and hence affect the speed of electromagnetic radiation. It determines the strength of recorded wavelengths within the electromagnetic spectrum (Duggin, 1985). Aerosols particles, such as pollution and dust, and skylight are considered to be most important optical parameters to be taken into consideration (Bowker et al., 1985).

To use remote sensed data for further analysis, it is advisable to go through atmospheric correction analysis to suppress the atmospheric effects to minimum (Curran & Novo, 1988). There are several correction methods, that have their own advantages and disadvantages (for example Mahiny & Turner (2007)). User should be aware of it when choosing the method/s, based on one's used material and purpose of study.

2.3.2 Optical properties of surface water

With remote sensing equipment, it is possible to measure water depth, but also in addition to that water temperature, organic and inorganic substances and spatial extent (Jensen, 2014). The basics of receiving total radiance (L_t) measurements from water is based on a function (Legleiter & Roberts, 2005), from four sources of electromagnetic energy:

A) atmospheric scattering, (L_p), resulting from downwelling sun and sky irradiance, but never reaches the water surface nor water body

B) water-surface radiance (L_s), that reaches only few millimeters of water body and is then reflected from water surface

C) Subsurface volumetric radiance (L_v), that penetrates to water body and reflects the material in it but does not reach the bottom

D) radiance from the bottom (L_b), as in the radiance, that penetrates through the water body all the way to the bottom and propagates back through the body and out of it.

The total radiance is hence calculated as followed:

$$L_t = L_p + L_s + L_v + L_b \quad (2)$$

but usually, studies are interested in some parts of the radiance components, as in this we are interested of the bottom radiance, for example. Isolating the pursued component as followed:

$$L_b = L_t - (L_p + L_s + L_v) \quad (3)$$

will give the wanted result.

These formulas may be represented with minor differences in labelling in different scientific sources, but what Jupp et al., 1985 added in their research of imaging reef was atmospheric transmission (T_a) as followed:

$$L_t = L_p + T_a\,(L_s + L_v) \quad (4)$$

specially for the radiance recorded at the satellite (see how atmosphere affects electromagnetic radiation in previous chapter, 2.3.1). In short, functions L_p, T_a and L_s are representing the variables that generally decreases the quality and effectiveness of remote sensing, and the radiance from variable L_v and L_b (Jupp et al., 1985).

Add some graphics to explain the chapter so it is more understandable.

2.3.3 Water quality

What is to be taking into consideration also is to acknowledge the pureness of the water column investigated. Seldomly natural aquatic systems are pure waters, as in free from all organic, e.g. phytoplankton, and inorganic, e.g. suspended minerals material. The state of the water quality can be assessed with subsurface volumetric radiance information (L_v). The suspended material decreases usually the farther from shore, and hence is rarely no significant concentration target on deep sea remote sensing. However, in inland and nearshore study areas the impact of suspended material can play a significant role as investigating the spectral reflectance of the water body (Miller & McKee, 2004).

The particles in water column increases reflection of light energy, and waves can either increase or decrease it. Winds and waves can also increase erosion and so the suspended material in the water column. Wind, rain and terrain slopes carry material from various sources into the water, increasing the turbidity.

Phytoplankton and zooplankton carry carbon (C) in them. Phytoplankton uses carbon dioxide (CO_2) to produce oxygen (O) as a result of photosynthesis. As they die, they sink to the bottom not releasing the carbon, but it sinks with them and bury under other sediments. Water bodies work as carbon sinks beside vegetation and soil, but unlike the latter ones, water bodies do not release CO_2 as frequently to the atmosphere as carbon sinks on land by e.g. decomposition and burning. However, the knowledge and studies reflecting the amount of carbon accumulation in global inland waters (and oceans) is still very scarce (Vachon et al., 2021).

2.3.4 Energy and light penetration in a water column

For receiving any kind of information of the water column, energy transition is a necessity. Energy transfers knowingly by three modes: conduction, convection and radiation (Kairu, 1982). In remote sensing, the energy transmission through radiation by electromagnetic waves is the essential part of producing information. In electromagnetic radiation the energy package, known as photon E (in units of joules, J), is travelling at the velocity of light in a vacuum-like space in wave-like pattern. For

every photon it is possible to calculate specific characterization (Bukata et al., 1995; Kairu, 1982) with

A) energy (E),

B) wavelength λ (meters, m), which is determined by the amount of time in which the light acceleration occurs,

C) frequency ν (cycles, s^{-1}), which is determined by how many accelerations occurs per second,

D) the velocity of light in a vacuum c, and

E) Planck's constant h after Planck, 1901,

with following relationships:

$$E = h\nu = \frac{hc}{\lambda} \quad (5)$$

and

$$\lambda = \frac{c}{\nu} \quad (6).$$

It is worth to mention, that standardized unit for wavelength is indeed meter, but sometimes expressing the wavelength is more convenient with nanometers (nm) or in micrometers (μm) (Bukata et al., 1995).

As it has been mentioned earlier on this chapter, when the energy penetrates through a water column, it undergoes scattering and absorption occurrences. The impact of them is depending on the quality of water and the presence of substances. Scattering and absorption of distributed radiance not only reduce the intensity of it, but also changes its directional character (Bukata et al., 1995). A shorter-wavelength light, for example blue and green light, can penetrate deeper into the water than longer-

wavelength light, like red light. This is because shorter wavelengths are scattered and absorbed less by water molecules, making it possible to penetrate deeper. For example, blue light can penetrate up to 100 meters in clear ocean water (that is why it appears as blue, but it also reflects the colour of a sky), while red light can only penetrate a few meters (for example, dystrophic lakes appear as dark brown caused by the dark organic matter, humus).

2.3.5 Sediment

When understanding how electromagnetic radiation interacts, in context of remote sensing, with sediment on the river bottom, monitoring environmental conditions, sediment properties and composition can be considerably less time consuming, cost effective and more constant. Remote sensing instruments gather information of the sediment from spectral reflectance, grain size and texture, mineral composition and moisture content, that all response to electromagnetic radiation either by scattering, absorbing, fluorescing, polarizing, transmitting and/or penetrating (Campbell et al., 2022).

Sediment underwater does not mean only the sediments at the bottom, but also the suspended and dissolved materials in the water column. Suspended sediments are inorganic particles in suspension within water (Curran & Novo, 1988). The suspended sediment concentration (SSC) is measured by the interaction of incident energy radiation (solar) with subsurface water material, which results as increase in remotely sensed spectral radiance ($L_{(\lambda)}$) returned to the sensor. Sediment properties, such as size, colour and mineralogy determines the relationship between SSC and $L_{(\lambda)}$, which is usually a positive correlation (Curran & Novo, 1988). Meaning, the more sediment in suspension, the higher the reflectance in the visible and near-infrared proportion of the electromagnetic spectrum (Curran & Novo, 1988; Ritchie et al., 1976, 2003).

2.4 Remote sensing

Remote sensing is data acquisition and observation method, that is done without a physical contact – remotely (Bukata et al., 1995; Goetz et al., 1983; Lintz & Simonett, 1976). Measurements are usually taken by a sensor device attached to another (moving) device or used the sensor independently. The data can be acquired from air, for example with aircrafts and satellites, and from ground, for example with thermometers and other ground-based sensors.

The first from of remote sensing for mapping and surveying purposes was aerial photography. Knowingly, the first aerial photograph was taken in 1858 from a balloon (Amad, 2012; Campbell et al., 2022; Goetz et al., 1983). After other kinds of sensors, for example imaging radar, made their advancements in the field, the term 'remote sensing' became more generally used and accepted (Goetz et al., 1983). It was World War I (1914–1918) that started the acquisition of aerial photography as a routine basis, and by the end of World War II (1939–1945) the techniques had developed greatly, by skilful experts and sensor equipment (Campbell et al., 2022). However, it was only the launch of the first Landsat satellite in 1972 that is considered as the start of modern remote sensing. Satellite imagery brought possibilities to image larger areas at once with narrower subtended angles and sun-synchronous orbit, which made the imaging of Earth's surface consistent at global scale (Goetz et al., 1983). Rising use of multispectral scanners and radiometric techniques allowed the correction of reflection effects on water surface and the recognition of bottom features more efficient than aerial photography, although it is capable of providing quite useful qualitative information on for example water depth and benthic algal biomass (Lyzenga, 1978).

The techniques that are accepted under the concept of remote sensing are based on emittance and reflection of electromagnetic energy (Bukata et al., 1995; Goetz et al., 1983). Therefore, for example measurements based on magnetism and gravity are not considered as remote sensing, even though the techniques require also no physical contact with the target.

Remote sensing methods can be divided into passive and active remote sensing data acquiring methodology (Jawak et al., 2015). The passive remote sensing methods are based on passive sensors, that detect radiation from natural source of light reflected

from surface from visible and invisible light spectrum. The active remote sensing methods on the other hand do not require any kind of source of light to distinguish information from the surface of the Earth but emits its own artificial light and radiation. Bathymetric remote sensing methods can also be divided into imaging and non-imaging methods, which are based on reflection values on a pixel or digital numbers (DN) or wave pulses from the sensor to the ground, respectively (Jawak et al., 2015).

2.4.1 Passive remote sensing

Passive remote sensing type uses optical, multispectral sensors (MS) and hyperspectral sensors (HS), which measures naturally available energy, for example the light from the sun. The sensors detect electromagnetic radiation's (EMR) intensity and wavelength, that is either reflected or emitted from the surface of a target. By analysing the reflected radiation, it is possible determine the depth of the water column based on the amount of light that is absorbed or scattered by it (Jawak et al., 2015). This is because different wavelengths of light are absorbed or scattered differently depending on the depth of the water and the composition of the water column, which was explained more profoundly in chapter 2.1.

All the passive remote sensing types are imaging methods, meaning it uses visible and/or invisible near infrared (NIR) light and microwave radiation. The reflected, visible energy are red, green and blue light, and the invisible reflection comes from NIR light. The emitted energy is for example thermal infrared energy (Jawak et al., 2015). Passive remote sensing devices are for example spectrometer, radiometer, imaging radiometer, sounder and accelerometer (Kogut, 2020). Most used are various types of spectrometers and radiometers, that distinguish spectral bands. For example, various satellites provide Earth-observation satellite imagery data based on spectral bands.

Satellites are used to gather information about the planet's surface, atmosphere, and oceans, and in a variety of applications, for example as environmental monitoring (e.g. Pettorelli et al., 2014), weather forecasting (e.g. Isaacs et al., 1986) and source of help in achieving for example sustainable development goals (SDGs) (e.g. Song & Wu, 2021). Sensors that are attached to the satellites are detecting and measuring

different types of radiation, such as visible light, infrared radiation, and microwaves. According to Zhao et al., 2022 overview of Earth observation (EO) satellites and their performance, Landsat, Sentinel, MODIS, WorldView and Gaofen were most significant current EO missions, from which MODIS has at the moment the widest range of applications.

Satellite remote sensing involves the transmission of signals from the satellite to a ground station. The data received from the satellite can be processed and analysed to create images and maps of the Earth's surface, as well as to measure various physical properties of the environment, such as temperature, humidity (Isaacs et al., 1986), and vegetation cover.

2.4.2 Active remote sensing

In active remote sensing, the device sends out a pulse of energy, such as light, sound, or microwaves, and then measures the characteristics of the reflected or scattered energy. The characteristics of the reflected energy can provide information about the properties of the environment being observed, such as the composition of the surface, the height of vegetation, or the depth of water. There are three types of active remote sensing: lidar, sonar, and radar.

The usually used type of active remote sensing for measuring relatively shallow water bodies, such as rivers, lakes, and coastal waters is Light detection and ranging (LiDAR). Bathymetry measurements completed with LiDAR are referred as airborne laser bathymetry (ALB), or airborne laser hydrology (ALH) (Mandlburger et al., 2013). Sonar is usually used primarily in deeper underwater environments. It emits sound waves, ultra-sounds, and measures their reflection to map the seafloor or detect underwater objects. Radar on the other hand uses radio waves to penetrate through clouds and vegetation to measure surface properties such as soil moisture and surface roughness. It holds a poor performance and even incapability to penetrate deep into water, so that type is seldomly used in bathymetry (Fitzpatrick et al., 2020).

LiDAR emits different wavelength laser pulses. Green laser pulse is often used and preferred in shallow water bathymetry, as it is capable of greater penetration of the

water column and is less attenuated than near-infrared wavelengths (Kinzel et al., 2013). Green region of the electromagnetic spectrum has a wavelength of approximately 495 to 570 nm. It is placed in the middle of the visible spectrum (380 to 700 nm), between blue light with a shorter wavelength and red light with a longer wavelength. The water penetration depth of green laser pulses is limited to relatively shallow depths, usually less than 20 meters in clear water as a requirement. That is rarely realistic in natural waters (Guenther et al., 2000). However, when observing riverbeds, green laser pulse performs creditably. The depth to which the laser pulse can penetrate varies depending on several factors, including the wavelength of the laser pulse, the clarity of the water, and the angle at which the laser pulse enters the water (Guenther et al., 2000; Kinzel et al., 2013).

2.4.3 Techniques of bathymetry

Conventional bathymetric measurement methods for estimating bottom surface have been single beam echo sound (SBES), multi-beam echo sound (MBES), and LiDAR (Evagorou et al., 2022). The measurements are achieved by installing the measuring device into for example boats, aerial platforms, remotely controlled or autonomous underwater vehicles (Janowski et al., 2021). The limitations in these are rather small spatial coverage, although the spatial resolution and accuracy is particularly high. Recent advantages in satellite-derived bathymetry (SDB) techniques have proved itself to be rather cost-effective and able to monitor large spatial coverage and is an advantage especially in remote and hard-to-get areas. Satellites can also provide continuous data frequently (Evagorou et al., 2022; Jawak et al., 2015).

2.5 Bathymetry

Bathymetry is the science of underwater topography (NOAA, n.d.). It measures the depth of all water systems: oceans, lakes, rivers, with remote sensing devices (Gao, 2009; Jawak et al., 2015). As one of the most basic forms of hydrographic data it provides essential information for environmental monitoring, navigation and mapping.

The measurement technique in bathymetry is based on energy transition in a water column, as explained in part 2.3. The energy can be for example a light or a sound penetrating a water column to the bottom. A sensor device is usually placed on a boat or other vessel. Measuring the time that it takes for the energy to travel to the bottom and scatter back, the depth and shape of the water element bottom can be determined (Campbell et al., 2022). Together with nowadays accurate, modern side-scanning sonars, bathymetric analysis performs even more reliable results when multiple sources of depth measurements are applied. Depending on study target's characteristics, suitable methods can be put in action. For example, for very shallow waters it can be difficult to place vessel to use acoustic instruments, but using aerial imagery meets the requirements.

Lyzenga algorithm and green band penetration into water better than other bands? (different depths)

Depth measurements based on visual capacity, for example Secchi disk measurements, do not tell the absolute depth of a water column, but the depth of visibility. It usually indicates of the water turbidity, as explained in part 2.3.x, which also affects the remote sensing energy transitions.

There are several applications to which bathymetry can be used and applied. The main applications are environmental monitoring (e.g. El Mahrad et al. (2020)), resource management (e.g. Orange et al. (2022)), sustainability monitoring (e.g. Zheng et al. (2022)) navigation (e.g. Elmore & Steed (2008)), disaster management (e.g. Zhou et al. (2021)), and military purposes (e.g. Wölfl et al. (2019)).

3 Study area

The study area takes place in the border line of northern Finland and Norway, at Tana (*Tenojoki* in Finnish) and its tributaries, located between 69°28'1.92"– 70°23'35" N and 25°50'37"– 28°12'59.76" E (WGS84) (figure x, see more detailed information in tables 1 and 2). In September 2022 a group of scientists took measurements from eleven 50m x 50m sites along the river and its delta sites from the upper reaches (Karigasniemi) to the lower reaches, almost to the Tanafjord. From those 11 sites two were selected for further examination for this thesis work. The two sites are Utsjoki, near Holiday village Valle, and Nuorgam, near Nuorgam elementary school (figure x). They represent two different parts of the large sub-arctic river by physical and fluvial characteristics, upstream and downstream, respectively.

3.1 Tana river

Tana is circa 361 km long frontier river outlet between Finland and Norway, that enters the Barents Sea at Tanafjord (Collinson, 1970; Eilertsen & Corner, 2011) (ELY Centre for Lapland, 2014) into the Arctic Ocean. Its source starts nearby of Karigasniemi, a village in northern Finland, from the confluence of 153 km long Anarjohka (*Inarijoki*) and 166 km long Karasjok (*Kaarasjoki*). Its drainage area is approximately 16 380 km^2 with high spring period (spring floods) and low winter period (frozen) discharge, > 500 $m^3 s^{-1}$, and < 70 $m^3 s^{-1}$, respectively (Eilertsen & Corner, 2011). Rather rapid water surface fluctuation is typical for the river impacting for example local salmon fishing. Tana is the largest and most productive natural salmon river in northern Europe (ELY Centre for Lapland, 2014).

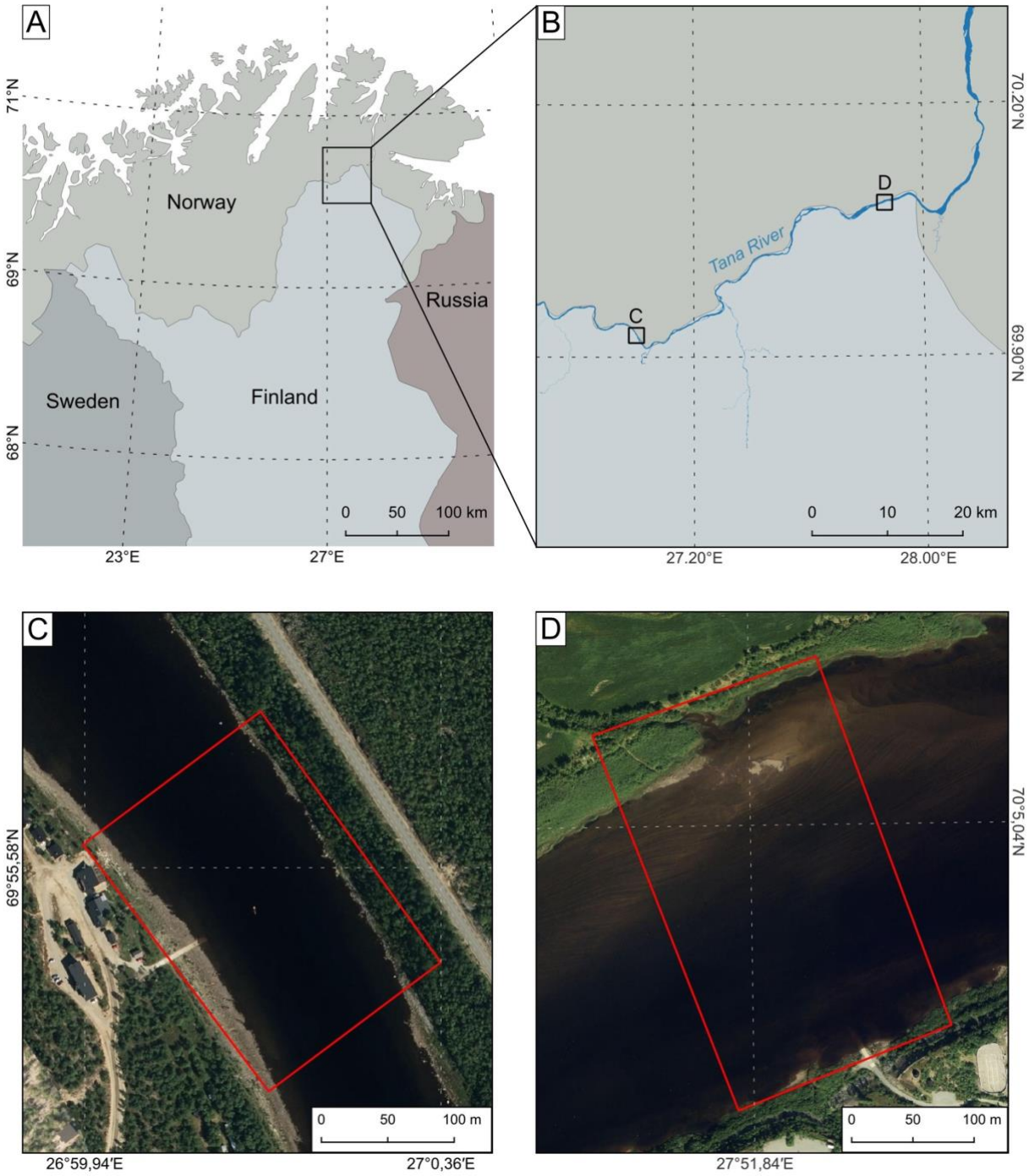

Figure x. (A) The study area is located to the border of Northern Finland and Norway, near Tana River's lower reaches. (B) The locations of the two study sites along the river. (C) Utsjoki study site, representing the downstream part, and (D) Nuorgam study site, representing the downstream part of the river. Aerial imagery in C and D is obtained from Norwegian Mapping Authority ©Kartverket, www.norgeskart.no.

3.1.1 Geomorphology

Tana river sediments consist of fluvioglacial material, older fluviatile and glacio-marine sediments. It is characterized by a relatively steep gradient, rapid flow, and a complex network of braided channels. After Lax et al. (1993), the Tana is divided into three parts based on the rivers geomorphology and flow rate. Upper Sand-Tana (*Ylempi Hiekka-Teno*) reaches from upper reach of the river to the other of the two biggest rapids in Tana, Karrakuoikka (*Yläköngäs*). Rapid-Tana (*Koski-Teno*) covers parts of the river from Karrakuoikka to Vuollegeavŋŋis (*Alaköngäs*), the other big rapid in Tana. Lastly, Lower Sand-Tana (*Alempi Hiekka-Teno*) starts from Vuollegeavŋŋis and ends to lower reach of the river forming a sand delta in Tana Bru (Lax et al., 1993) (figure x). The middle part of the river, Rapid-Tana, consist of bigger rock shores and various size of rapids, as the other two parts consist of sandbars and shallower, slow flow-rate parts of the river (Lax et al., 1993).

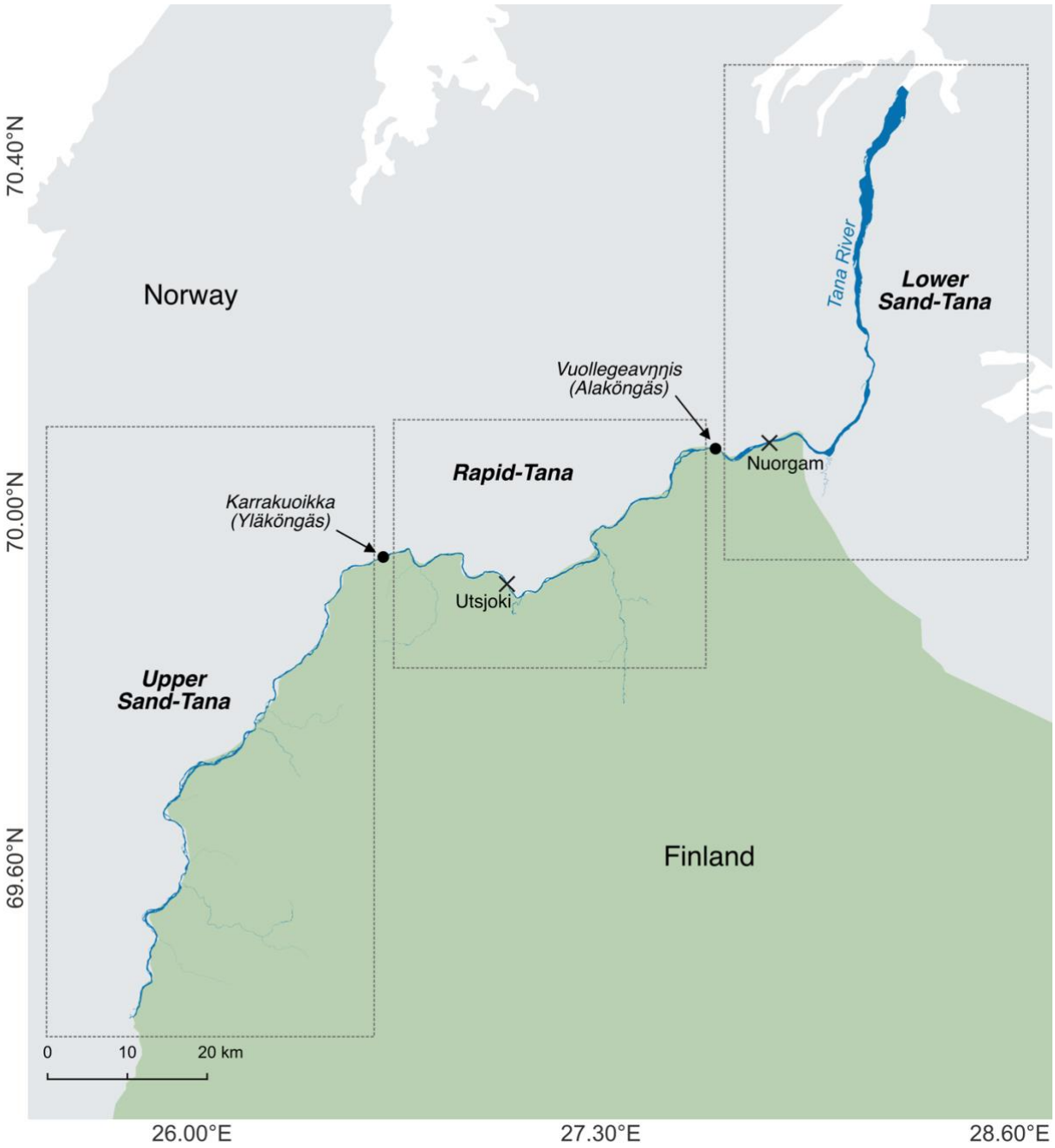

Figure x. Tana river's geomorphological division after Lax et al. (1993). The dots represent the locations of two big rapids, Karrakuoikka and Vuollegeavŋŋis, that acts as dividers for fast flow-rate Rapid-Tana and sandy slower flow-rate parts of the river. The X symbols denote the locations of the study sites.

The river is highly influenced by the geology of the region. The bedrock in northern parts of Finland and Norway are under the domination of hard, crystalline rocks of the Fennoscandian Shield (Nironen, 2017), that are resistant to erosion. Because of it, the river has cut into the landscape, creating steep valleys and gorges. The valley depth vary from 80 meters up to 300 meters deep (Mansikkaniemi, 1970). The downstream of Tana increases its depth compared to the upper course of the river,

but the width remains quite the same in the upper course as in the lower course (Mansikkaniemi, 1970).

The river has a relatively high sediment load, which is transported downstream and deposited in the lower reaches of the river. At the lower course of the river, the sediments consists mostly of sand, silt and clay, and is quite erodible (Collinson, 1970; Mansikkaniemi, 1970). The main physical factors controlling the erosion and other modifications in the riverbed are wind, waves and changing currents. The magnitude of those impacts depends on local morphology, slope and on the duration and strength of the wind (Collinson, 1970). River geomorphologies in northern high-latitude regions are facing changing conditions due to rapid climate change impacts compared to global average (Huang et al., 2017), as for example precipitation is expected to increase, and ice-cover periods are expected to shorten. These actions impact for example sediment transportation (Lotsari et al., 2022).

3.1.2 Climate and hydrology

Weather and/or climate factors impacting and limiting the quality of remote sensing are amongst other things precipitation, cloudiness, snow and ice cover and the amount of light. Tana is upon a sub-arctic climate. It is categorized after Turcotte et al., 2011 classification as freshet-dominated river, which includes river characterizations such as insignificant snowmelt during winter months, stable ice conditions, annual minimal late-winter runoff, and subzero temperatures through winter time. The climate conditions are in general described as more continental as usual in relation to its location due to the combined effects to climate from the Gulf Stream and the Barents Sea (Lotsari et al., 2010).

The annual precipitation is approximately 700-800 mm and is mostly received as falling snow during the winter months. Mean temperature is –0.7 °C. Closer to the sea more there is annual precipitation, up to 940 mm. The river freezes usually in November or late October and stays frozen approximately seven months. Discharge takes place a month after the breakup of ice, usually in early June, but sometimes already in May. The river run-off stabilizes for most of August after the flooding of

about 110-160 m^3/sec (Collinson, 1970). As the snow melts in the spring and early summer, it releases water into the river.

The hydrology of Tana is important for the culture of the region for a variety of reasons. The river has considerable role in supporting fish populations (for example Atlantic salmon population complex), in fishing industry and tourism (Fossøy et al., 2022; ELY Centre for Lapland, 2014). The river and its environment have also significant history and meaning for local Sami culture, from traditional fishing habits to ancient monuments. The whole catchment area has experienced considerably little anthropogenic impacts and is so a relatively unique river system.

4 Materials and methods

The comparison is made by evaluating the qualitative performance of each model and accuracy of different models of bathymetric mapping. This study compares three methods to conduct bathymetric models: multibeam sonar, acquired using autonomous surface vehicle (ASV), aerial laser scanning (ALS) and satellite imagery from Sentinel-2 satellite. In addition to these comparisons, the qualitative performance is evaluated, how the models perform under different hydrological conditions caused by weather, location on river (downstream and upstream), and season. Along with detecting the differences, evaluating the models and stating their strengths and weaknesses are also in the center focus of this study.

The data are high quality but has their limitations and errors. In ASV data, in Utsjoki study site, the material is after manual and automated filtering (more about the pre-processing in chapter 4.1.1) and modelling striped so to speak, that impacts the quality a little bit, but altogether not the analysis. In Nuorgam study site, there were areas on the outer edges that were scanned only once, which affects the area's accuracy. However, there is an area that is by its coverage sufficient for decent analysis. In addition, both study site's data should go through a proper patch test to cover possible errors caused by roll that GPS/INS could not correct, but for that process the data is not in right format to go through it. In ALS data pre-processing, done in National Land Survey of Finland (NLS), the calibration of the sensors was not optimal, and the trajectory data did not quite overlap each other, but other than that the laser scanning data is quite workable.

In tables 1 and 2 there are listed primary physical factors of weather in the study sites on given days of surveys: in table 1 there is the weather conditions in Nuorgam study site, and in table 2 Utsjoki. The values of air temperature, precipitation and wind velocity have been acquired from Finnish Meteorological Institute (FMI) open-source data online service (https://www.ilmatieteenlaitos.fi/havaintojen-lataus). The observation frequency was at its most between 10 minutes in a day, so mean values were calculated to represent the average figures. Flow rate information was acquired from online water information service centre (https://www.vesi.fi/karttapalvelu), under the maintenance of the Finnish Environmental Institute (FEI). The flow rates were daily observations, but as Sentinel-2 imagery data composes of image collection

from multiple days, a mean value of flow rate was calculated for the sake of comparison.

Table 1. Data of Nuorgam: data acquisition dates, weather conditions and locations.

	ASV	ALS	Sentinel-2	Validation data
Date time	17.09.2022	07.09.2022	01.07.2022 – 14.07.2022	17.06.2023
Latitude (N)	70°4’56’’ – 70°5’2’’	70°4’54’’ – 70°5’6’’	70°4’54’’ – 70°5’6’’	70°4’56’’ – 70°4’57’’
Longitude (E)	27°51’50’’ – 27°52’1’’	27°51’38’’ – 27°52’5’’	27°51’38’’ – 27°52’5’’	27°51’56’’ – 27°52’1’’
Air temperature (mean)*	6.95 °C	5.53 °C	15.73 °C	20.68 °C
Precipitation (mean)*	0.18 mm	0.00 mm	0.17 mm	0.00 mm
Wind velocity (mean)*	2.67 m/s	1.31 m/s	2.02 m/s	2.05 m/s
Flow rate**	187.9 m^3/s	147.3 m^3/s	160.6 m^3/s (mean)	155.3 m^3/s

* Utsjoki Nuorgam observation station (lat: 70.08, lon: 27.90), source: FMI

** Polmak observation station (lat: 70.08, lon: 27.90), source: FEI

Table 2. Data of Utsjoki: data acquisition dates, weather conditions and locations.

	ASV	ALS	Sentinel-2	Validation data
Date time	19.09.2022	07.09.2022	01.07.2022 – 14.07.2022	18.06.2023
Latitude (N)	69°55’31’’ – 69°55’36’’	69°55’29’’ – 69°55’38’’	69°55’29’’ – 69°55’38’’	69°55’32’’ – 69°55’33’’
Longitude (E)	27°0’1’’ – 27°0’14’’	26°59’56’’ – 27°0’21’’	26°59'56’’ – 27°0’21’’	27°0’2’’ – 27°0’6’’
Air temperature (mean)*	6.39 °C	4.75 °C	17.33 °C	19.95 °C

	ASV	ALS	Sentinel-2	Validation data
Precipitation (mean)*	0.01 mm	0.04 mm	0.12 mm	0.00 mm
Wind velocity (mean)*	6.16 m/s	1.57 m/s	2.90 m/s	2.80 m/s
Flow rate**	254.6 m^3/s	138.1 m^3/s	150.2 m^3/s (mean)	145.3 m^3/s

* Utsjoki Kevo observation station (lat: 69.76, lon: 27.01), source: FMI

** Onnelansuvanto observation station (lat: 69.91, lon: 27.02), source: FEI

4.1 Close-range and mid-range remote sensing data

The bathymetric measurements were obtained using two different remote sensing methods. One represents close-range method, which data was collected using autonomous surface vehicle (ASV), Maritime Robotics. Its bathymetric measurements are based to echo depth sounding technique. It's possible to integrate different types of measuring devices to the ASV, and its positioning system is based on RTK-GPS (Real Time Kinematic Global Positioning System) satellite positioning technique. More detailed information is described in chapter 4.1.1. The other remote sensing method, from mid-range, was using a helicopter, which measured the depth with laser beams (airborne laser scanning, ALS).

4.1.1 Autonomous surface vehicle data

The ASV measurements were taken in September, in Nuorgam study site on 17th and on Utsjoki 19th 2022. The sensor, Baywei multibeam echosounder, aka multibeam sonar was attached to the vehicle, Maritime Robotics, unmanned surface vehicle Otter. The RTK system used was Trimble Applanix Pos MV, which features in addition to RTK receiver, a high accuracy inertial measurements units, producing more robust georeferencing and accurate attitude in various dynamics, with no timing errors. The raw data (backscatter) from ASV was first decoded with QPS Qimera software from s7k format to xyz-dimension point cloud data. The horizontal

resolution of the point cloud is 25 cm in ETRS-TM35FIN (EPSG:3067) coordinate system. The pre-processing stage includes georeferencing of each sample point, which are derived from the information produced by the multibeam sensor and its ancillary sensor. That information includes the position and attitude of the vessel, location of the sonar head in the vessel, geometry of the beams and sound velocity of the water column (Schimel et al., 2018). Then a manual and automated clean-up filtering was implemented to remove outliers. The automated filtering was processed using “median spline filter”-algorithm. Total of 160 556 and 198 489 measurement points were measured from Utsjoki and Nuorgam study sites, respectively.

The weather conditions on study sites on measurements days were quite rainless and snowless. The temperature were around plus 6 to 7 Celsius degrees (see tables 1 and 2 for more detailed information). The wind velocity and flow rate were stronger on the 19th day, when measurements at Utsjoki study site were made. Utsjoki study site is on upstream at the Tana river. Nuorgam study site, at downstream, had more moderate flow rate and wind velocity (see tables 1 and 2). Utsjoki wind velocity was around 6 m/s, which means moderate breeze (on Beaufort scale), forming small, approximately one-meter-long waves.

4.1.2 Airborne laser scanning data

The ALS data was collected by a helicopter on 7th of September 2022. There were three sensors attached to the helicopter, from which the green laser beam is especially meant for mapping the river bathymetry. The other laser beams serve for the purposes scanning the environment above water.

The point locations were calculated straight from GPS/INS without ground control point marking. Usually, ground control points are necessity for accurate positioning in wanted coordination system, as GPS/INS alone is not accurate enough. In the data pre-processing some manual work was done correcting some of the trajectory’s elevation information. For this study the accuracy of the point locations is deserving enough. The finished point cloud data was delivered in LAZ format and the elevation information calculated to N2000 reference system, which stands for Finnish nationwide reference system to describe water elevation information. The system is based on the European spatial vertical reference systems European Terrestrial

Reference system 1989 (ETRS89) and European Vertical Reference System 2000 (EVRS2000). Hydrographic offices around Baltic Sea region have agreed to take use these common reference systems and named it Baltic Sea Chart Datum 2000 (BSCD) (Schwabe et al., 2020).

Compared to weather conditions differences between study sites on ASV data collection days, ALS data was collected in much more similar weather conditions in both study sites. Rain and wind velocity was quite non-existing, and flow rate was around 140-150 m^3/s (see detailed information from tables 1 and 2). This enables more stable and more free form disturbance and noise factors, as the water turbulence does not cause as much additional reflections to the water column, as it will affect the data collected with ASV, especially in Utsjoki study site.

4.2 Satellite imagery data

The satellite imagery data used in this analysis was Sentinel-2 level 2A, provided by the European Space Agency (ESA). The Copernicus Sentinel-2 mission was launched in June 2015. Global data provided by it has been available since 2017. It is equipped with large range of technologies supporting the Copernicus Land Monitoring studies, such as multi-spectral imaging instruments for vegetation, soil, water and atmospheric monitoring. It suites also for studying inland waterways and coastal areas. It is a wide-swath width, 290 km, and its spatial resolution varies from 10m, 20m, to 60m, depending on the wavelength. The MultiSpectral Instrument (MSI) has 13 bands: 4 visible, 6 Near-Infrared (NIR), and 3 Short-Wave Infrared (SWIR) bands. Its temporal resolution, aka revisit time is relatively high: at the equator 10 days with one satellite, and 5 days with two satellites. That results 2-3 days revisit time at mid-latitudes, under the same viewing conditions (ESA, n.d.).

For this study Sentinel-2 imagery from July 2022 was used (see tables 1 and 2 for more specific information), since it was the closest date to the closer-to-ground studies, when there was imagery available without clouds above the study sites. It is good practice that the satellite imageries from study sites are from same period in relation to the ground data acquisition time. The spatial resolution is 10 meter.

4.3 Ground point measurements

Ground point measurement data were taken 17th and 18th of June 2023 from the study sites for the validation analysis and accuracy assessment of the ASV, ALS and satellite imagery data and models produced from them. With Trimble R10 GNSS receiver device, 31 measurement points were taken from the shorelines of the study sites (figure x). The validation data applies in this study only to validate the accuracy of ALS data and satellite imagery, as the validation points do not quite reach the scanning area where ASV point clouds were acquired.

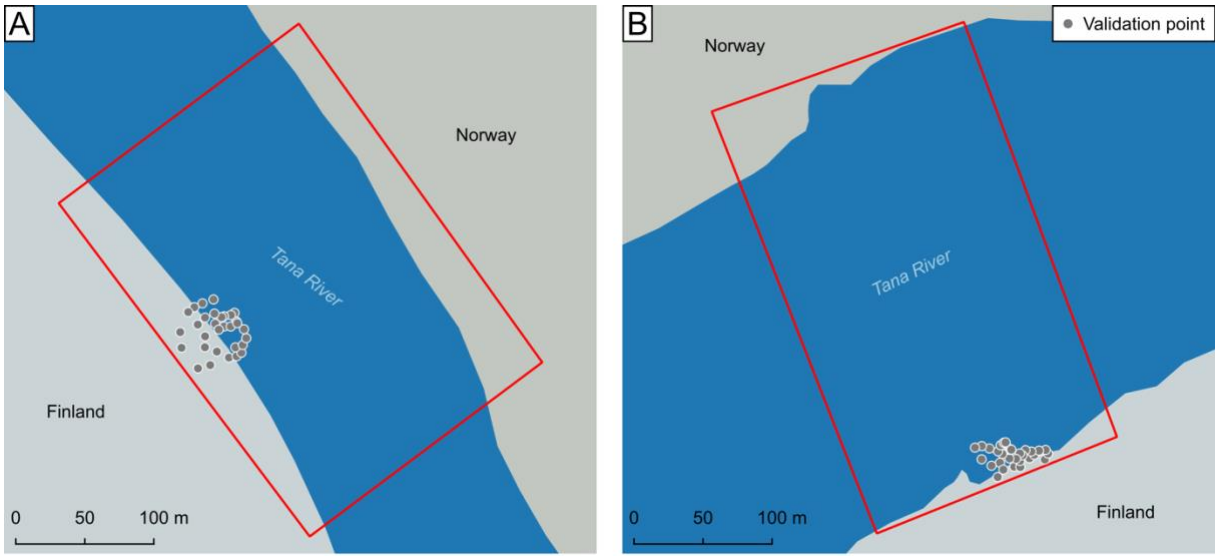

Figure x. Validation points in study area (A) Utsjoki and (B) Nuorgam.

4.4 Bathymetric modelling

As described in chapter 4 more profoundly, the dataset used in this study went through pre-processing before conducting complete bathymetric modelling. Both ASV and ALS data originate from point cloud data, which were interpolated with Inverse Distance Weighting (IDW). Sentinel-2 imagery obtained using Google Earth Engine.

Näistä kartoista tarkoitus tehdä uudet versiot

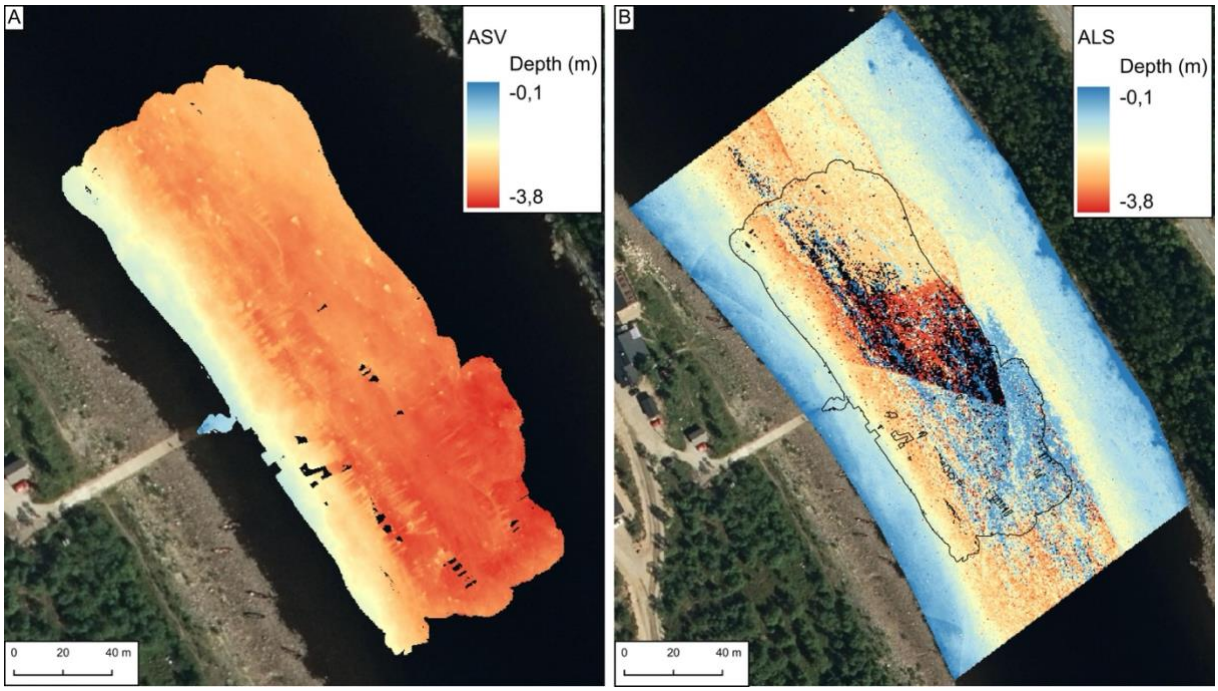

Figure x. (A) ASV bathymetric model of Utsjoki study site. (B) ALS bathymetric model of Utsjoki study site. In B image there is the outline of ASV set in proportion in area of DTM from ALS.

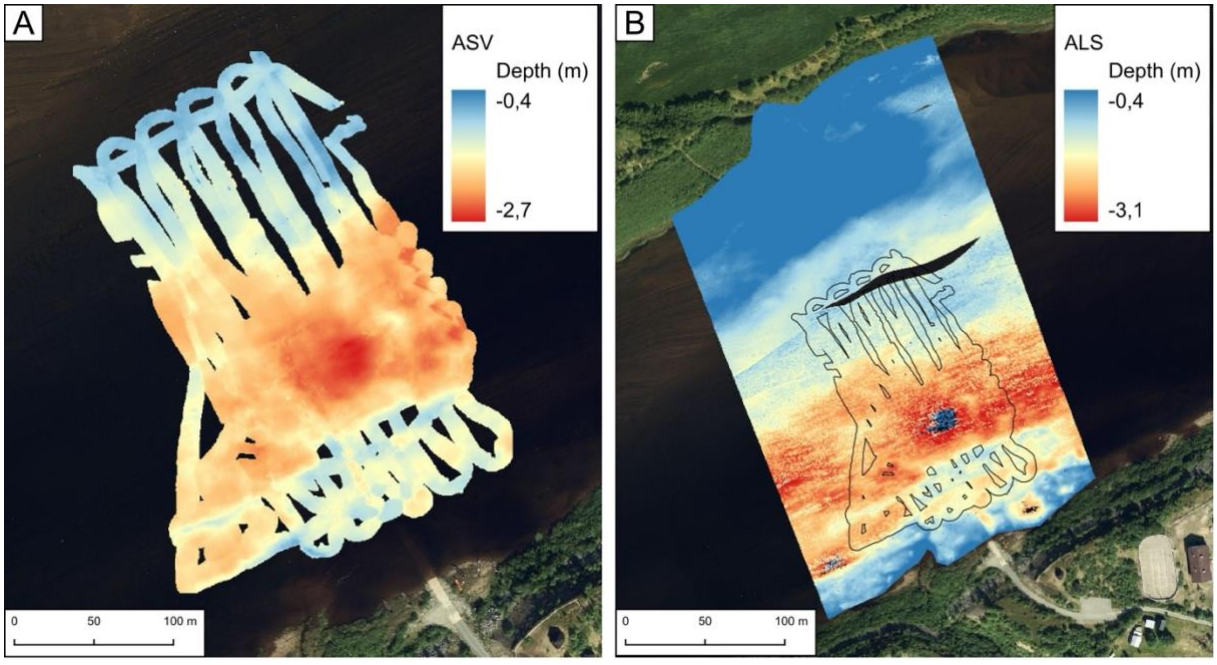

Figure x. (A) ASV bathymetric model of Nuorgam study site. (B) ALS bathymetric model of Nuorgam study site. In B image there is the outline of ASV set in proportion in area of DTM from ALS.

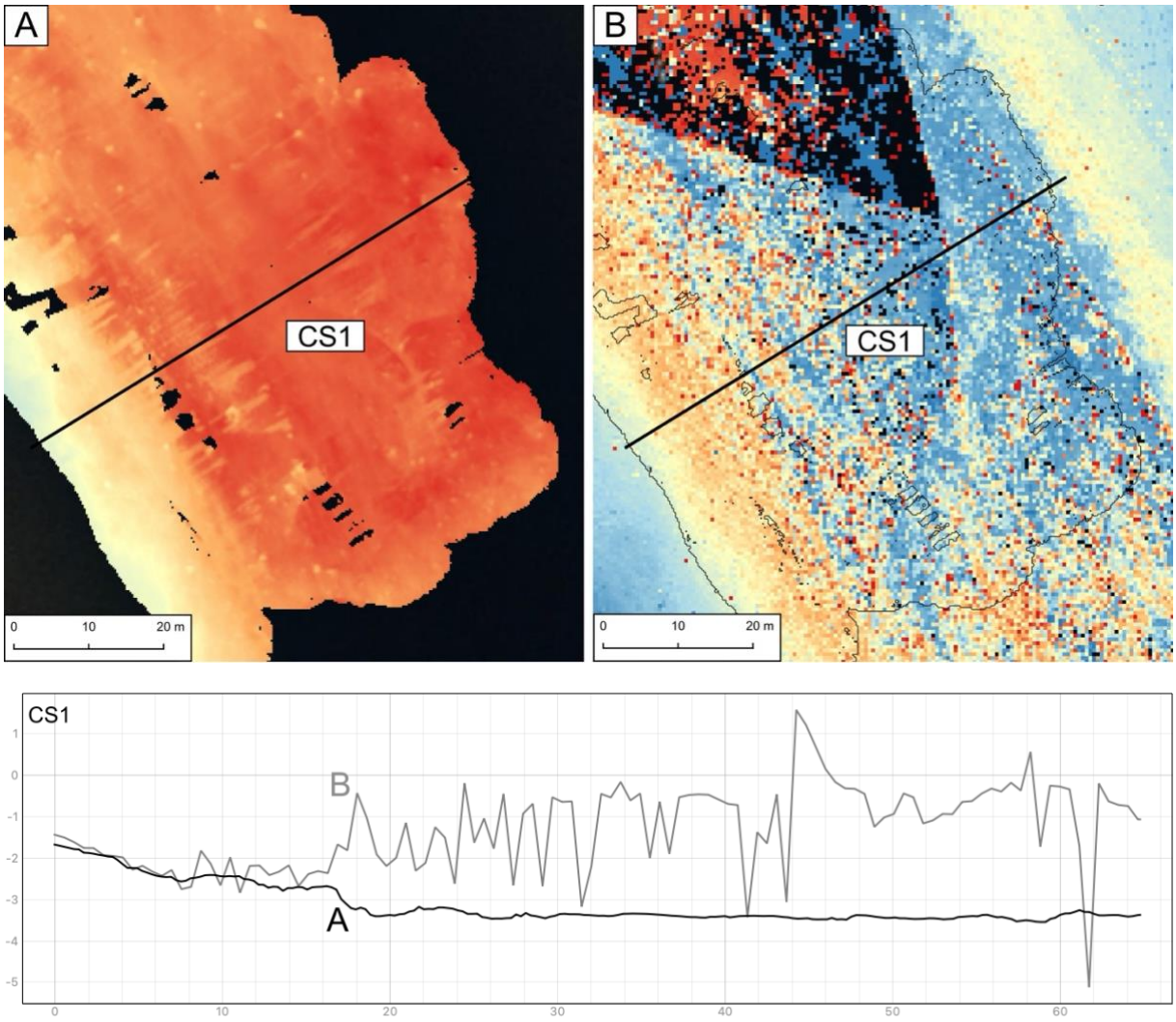

Figure x. Utsjoki cross-section 1 elevation profile. Closer to Finland's side shore the correlation is quite same, but the deeper depths cause much dissimilarities.

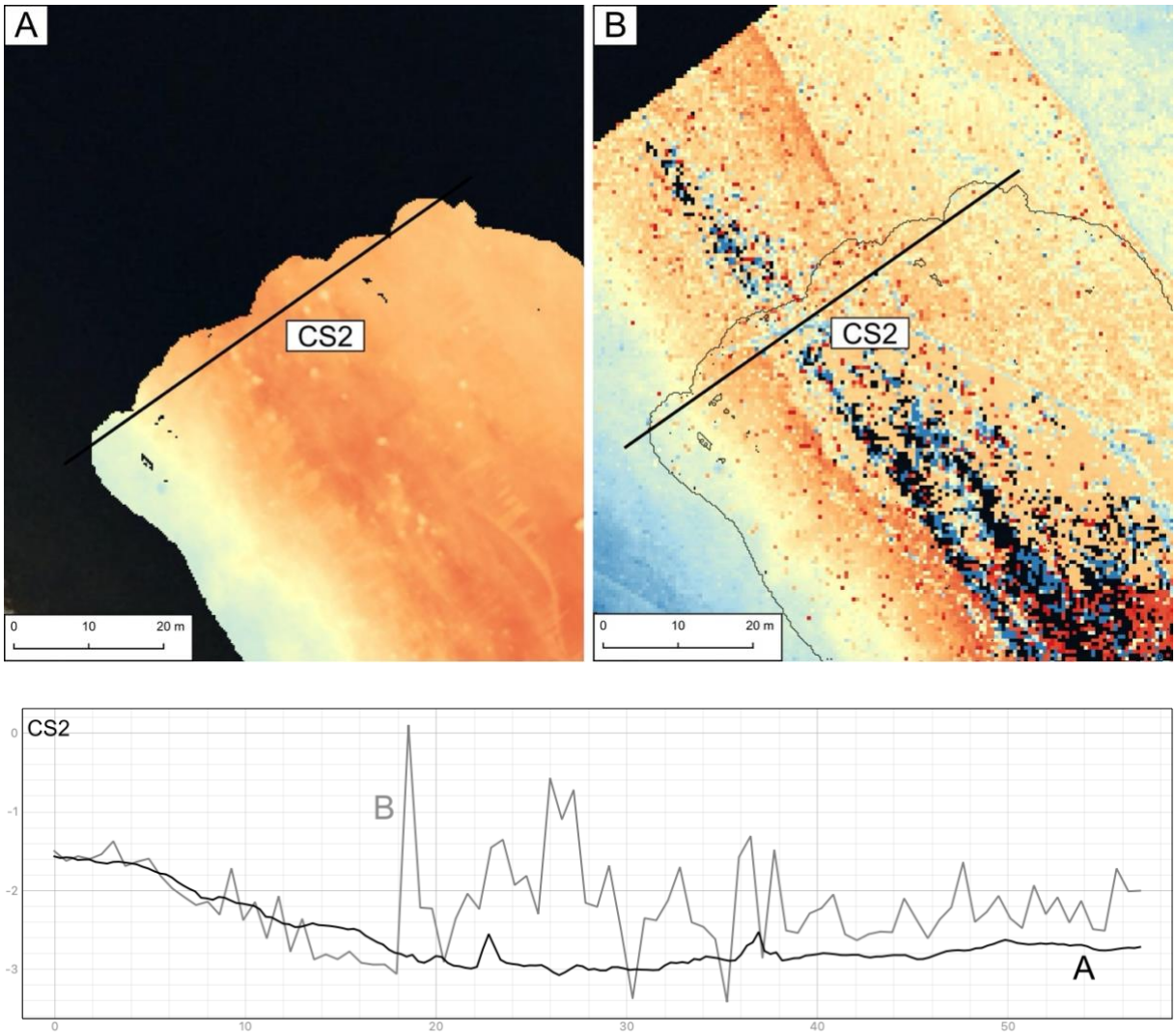

Figure x. Utsjoki cross-section 2. A little more corresponding elevation profile, but (B) ALS still exaggerate the elevation, but correlation is seen.

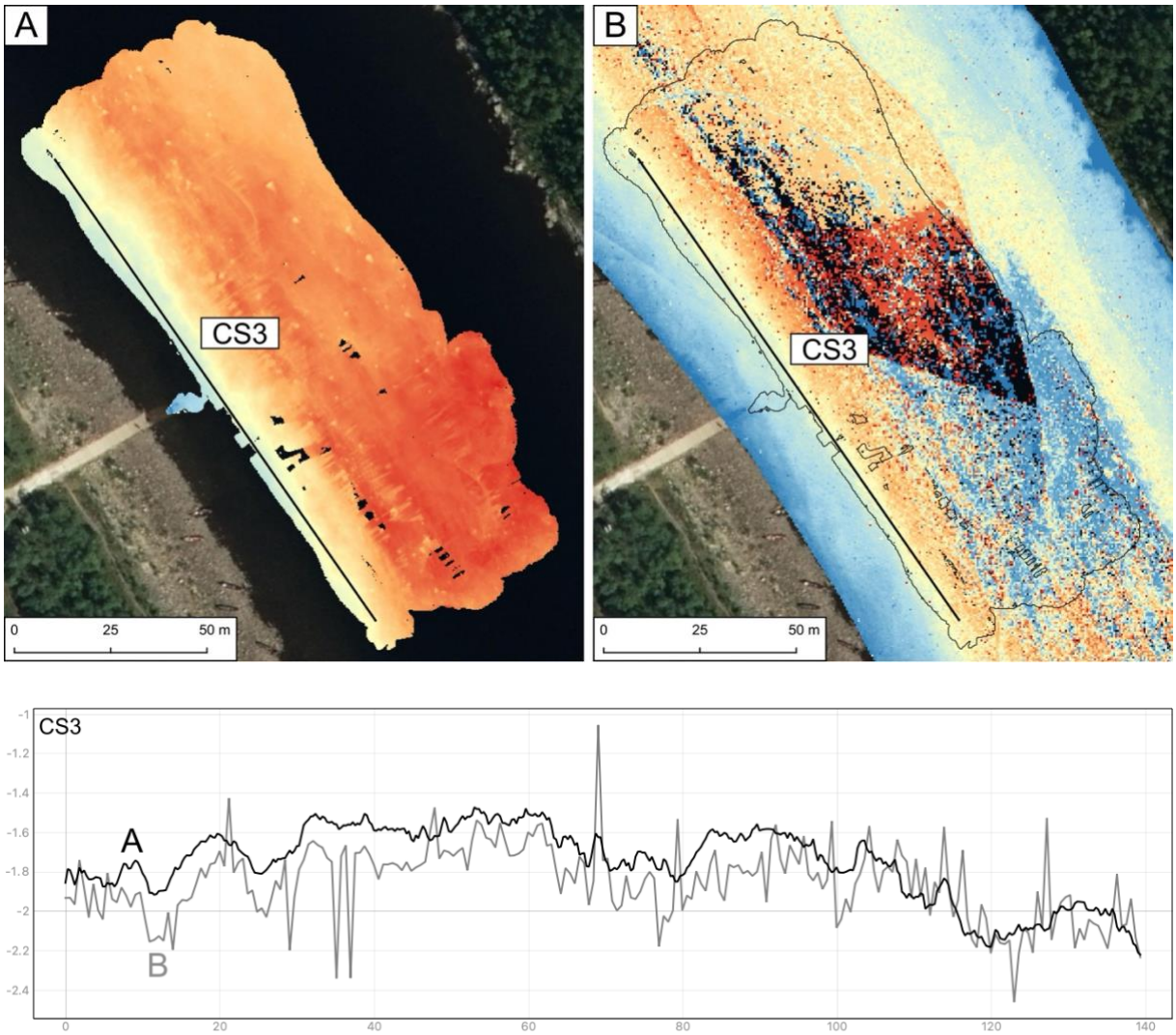

Figure x. Utsjoki cross-section 3.

Must explain what happens in the middle of ALS model

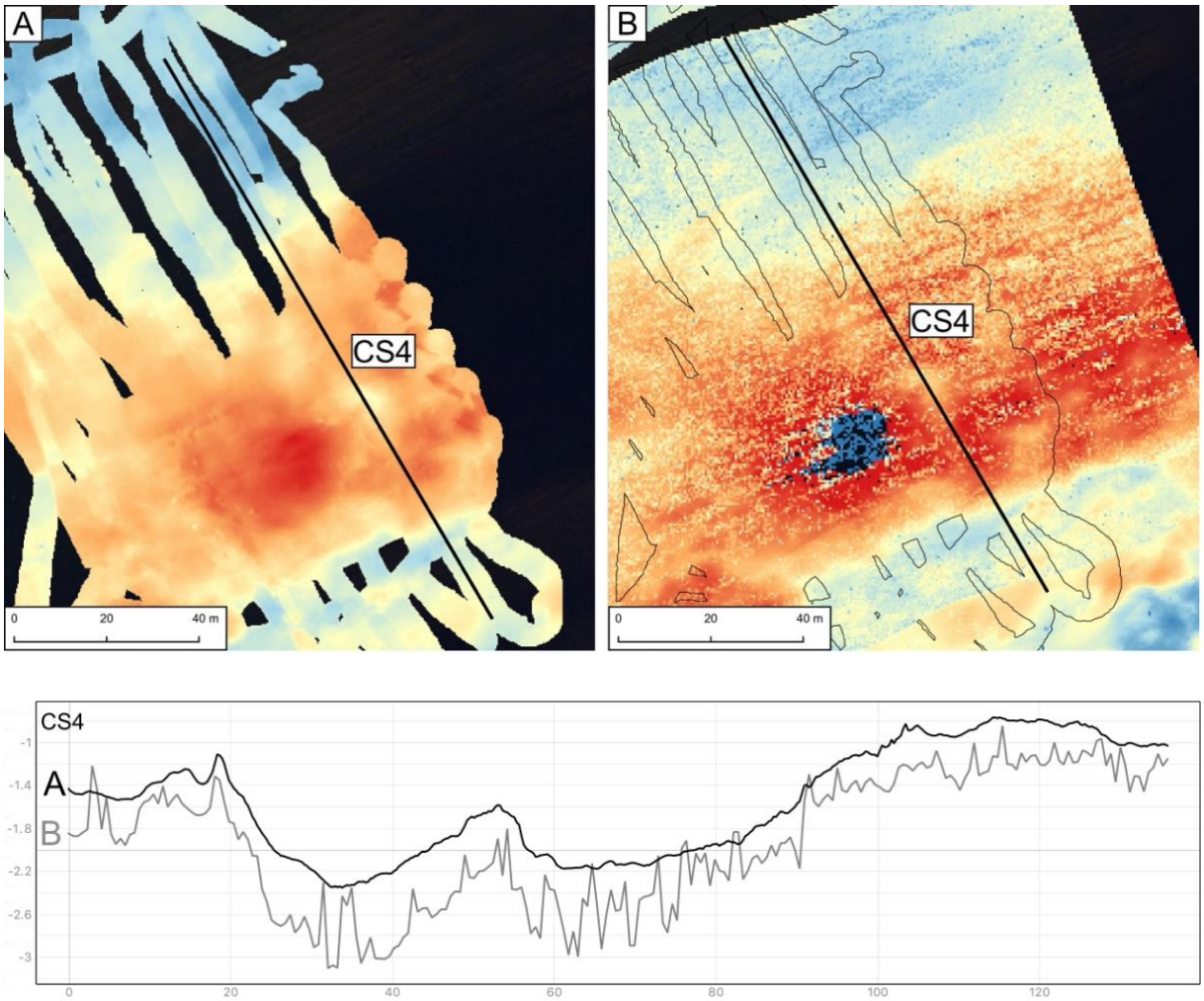

Figure x. Nuorgam cross-section elevation profile.

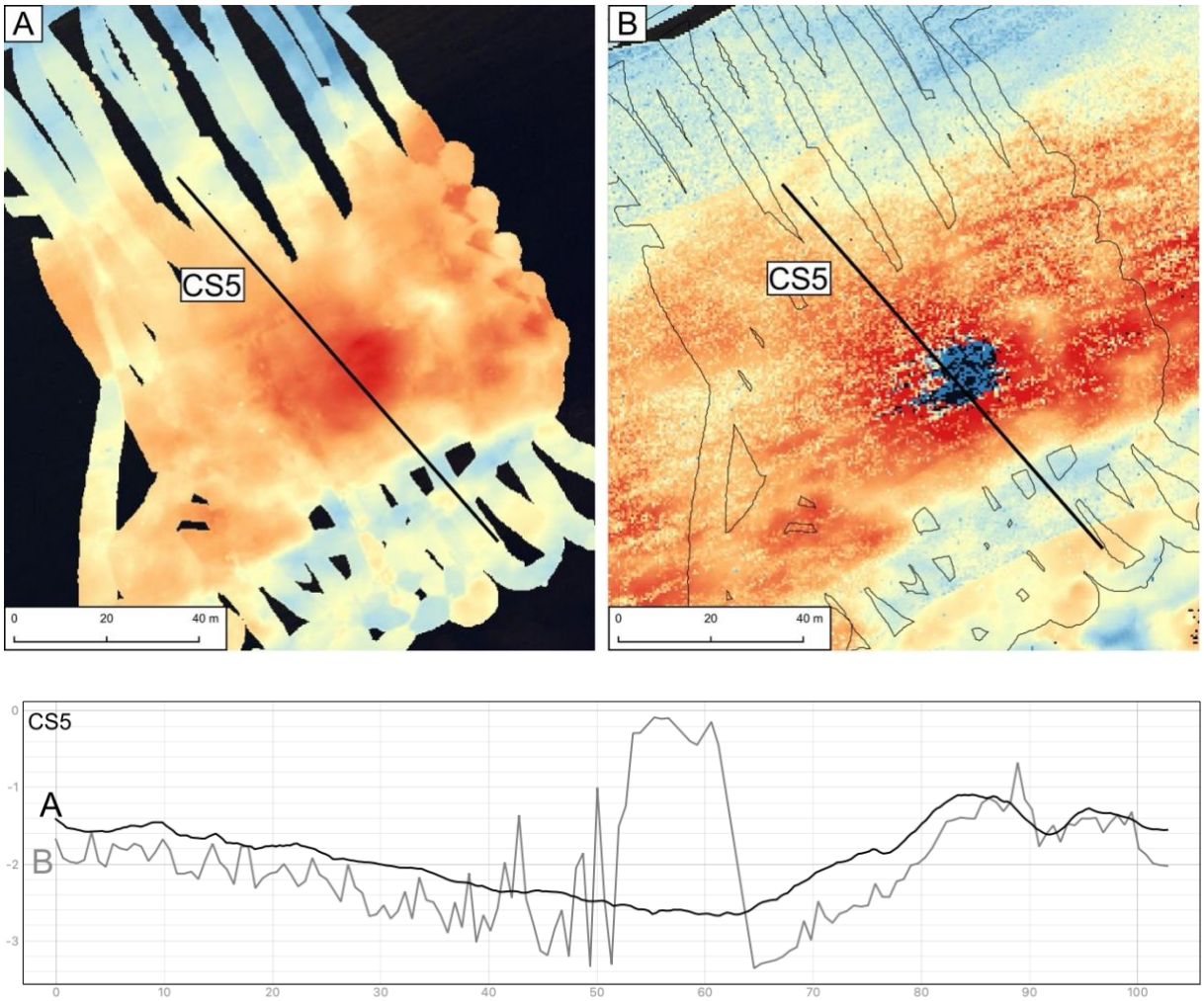

Figure x. Nuorgam cross-section.

Must explain what happens in the middle of ALS model

Qualitative evaluation of models:

- refer to cross-sections
- add vertical difference and roughness analysis
- add satellite analysis when ready

Quantitative evaluation:

- validation point and model correlation graphs and errors (table in chapter 5)
- outliers

4.4.1 ASV modelling

After data pre-processing described in chapter 4.1.1 the point cloud data was ready for further analysis in XYZ file format. XYZ file is a simple format for recording points geometry in 3D space – each column has its separate coordinate information: x-axis represents the horizontal line (east and west), y-axis the vertical line (north and south), and z-axis indicates height or elevation.

Utsjoki site has 160 556 xyz-points and Nuorgam site 198 489 points. Tana River is approximately (how many times bigger) at the site of Nuorgam than in Utsjoki site, but Utsjoki site was scanned more densely, meaning that same lines were scanned more than once, while Nuorgam site had parts which were scanned only once, leading for less dense scanned parts, which lacks less information of the bottom.

XYZ-files were imported to QGIS, a Free and Open Source (GIS) Software (FOSS), as point cloud data. Based on an assessment studies by Panhalkar & Jarag (2015) and Šiljeg et al. (2015) the output results of bathymetric modelling are highly dependent on multiple factors, like sample density, terrain features, data-gathering methods and interpolation methods. Panhalkar & Jarag (2015) studied different bathymetric models' performance in Panchganga River, India, where they completed Inverse Distance Weighting (IDW) performance as most accurate method for generating bathymetric model. Šiljeg et al. (2015) came to a solution in their interpolation method comparison study, that in following order, IDW, multiquadric function (MQ) and ordinary kriging (OK) resulted the best results modelling shallow shores of Lake Vrana in Croatia. In addition to these research result, as described in chapter 4.1.2, ALS was delivered in LAZ format, which with more specific description of processing in following chapter 4.4.2, was obtained to DEM with IDW, so in conclusion, ASV DEM were modelled using IDW interpolation method.

From the interpolated model no-data holes and on-way routes that the vehicle took while scanning the area were removed, as in clipped out, resulting the final model (see fig. xA and xA). From Nuorgam ASV interpolated model (fig. xA) the once took routes were not however clipped out, due to the small size of model it would have been resulted if they were to be clipped out. The sparse density of parts scanned only once are taken into consideration in the quality assessment. Both models were interpolated to resolution of 0.25m bathymetric raster.

4.4.2 ALS modelling

ALS data was delivered in LAZ format. LAZ, or LASzip file format is compressed LiDAR Aerial Survey (LAS) format used for restoring LiDAR point cloud data. Utsjoki site's point cloud consists of 1 771 687 points and Nuorgam site of 2 883 542 points. Utsjoki points has been classified into three categories: ground (44.5%), medium vegetation (18.3%) and unclassified (37.2%). Nuorgam points have two classifications: reserved (32.2%) and unclassified (67.8%).

LAZ files were first filtered from outliers and possible noise. Filtering (and later rasterizing) was implemented with Point Data Abstraction Library's (PDAL) pipelines. PDAL is an open-source library and applications for processing point cloud data written with C/C++. The point cloud processing contains composing operations into pipelines, that can be written in JavaScript Object Notation (JSON) syntax or using available application programming interface (API).

In Utsjoki study site the filtering range for z-axis was set up to values between 70 and 100, as the elevation (height) values in river bottom were around 80-90 (meters). Other values were considered inessential. Utsjoki site's elevation above sea level is around 60-70 meters, but LAZ-file delivered had elevation information calculated based on height measurement between GPS receiver and terrain. Nuorgam site had corresponding values 10 and 30, as elevation above sea level in Nuorgam study site is around 10-30m. Filtering elevation outliers out helps the digital surface modelling become more even and accurate for further analysis.

Rasterizing, that is generating DSM happens with GDAL writer, that uses IDW interpolation algorithm. Data type was defined to GeoTIFF. Resolution was set to 0.25, the same as ASV, and produced a fine-looking output.

After rasterizing LAZ-files the DSMs were brought to QGIS. The models were clipped to include only river area (fig. xB and xB), as the delivered area included data from shore bank as well, that is not essential information for this study.

4.4.3 Satellite imagery modelling

(Flener, 2013; Li et al., 2021; Said et al., 2018)

Lyzenga81 (Lyzenga 1981) attenuation coefficient ratio 0.9908802755591943. between green and blue bands.

Kalibrointipisteet asv-mallista, joiden arvot ovat samat kuin als-mallissa

Nuorgam correlates better than utsjoki, but they follow the same pattern as the correlations between asv and als ->Correlation between als and satellite
Validointipisteiden jako validointi- ja kalibrointinäytteisiin (ei toimi nuorgam koska validointipisteet ei yllä asv-malliin…)

4.5 Quality assessment of bathymetric models

Onko jo results-kappaleen asioita? Käydäänkö assessment-menetelmät läpi jo aiemmissa kappaleissa?

5 Results

5.1 Quantitative assessment

Validation data error assessment results

Table 3. The results of root mean squared, absolute and maximum errors and R-squared on IDW modelled river bottom DEMs derived from ASV data, compared to validation point data. N=31.

	Utsjoki ASV	Nuorgam ASV
RMSE	1.7838706318406874	1.1568474726087066
MAE	1.4331780161290262	1.0201863400000006
MAXE	4.261111999999997	2.3705827
R^2	0.44577947248012084	0.3421801604585336

Table 4. The results of root mean squared, absolute and maximum errors and R-squared on IDW modelled river bottom DEMs derived from ALS data, compared to validation point data. N=31.

	Utsjoki ALS	Nuorgam ALS
RMSE	0.16526257931156874	0.17681145003216284
MAE	0.12614583495443576	0.11840849070220001
MAXE	0.427248066521301	0.7277976715493999
R^2	0.981994064920988	0.9689414156757721

In table 3 and 4 there are the results of the interpolated model's validation analyses. -- IDW interpolation method, using 3 as a distance coefficient P value.

5.2 Qualitative assessment

The qualitative assessment of the performance of the models

Kohdat, joissa als rakeilee on matalammat kohdat -> matalammat kohdat joen käänteessä -> kohta ei niin meanderoiva, mutta sisäpuoli käänteessä virtaus hieman hitaampaa yleensä -> syvemmällä

virtaa kuitenkin enemmän vettä, enemmän pinta-alaa kuin matalalla -> liike + syvyys aiheuttaa häiriötä/meteliä?

Korrelaatio aika hyvä, als yleisesti tuottaa syvempiä tuloksia kuin asv -> oikeasti, vai laskuvirhe?

6 Discussion

6.1 Reference/reflection to main research objectives/questions

6.2 Interpretation of results (tulkinta)

6.3 Implications of this work in relation to other works

6.4 Limitations of the study

6.5 Recommendations for further research

7 Conclusion

References

Alho, P., Vaaja, M., Kukko, A., Kasvi, E., Kurkela, M., Hyyppä, J., Hyyppä, H., & Kaartinen, H. (2011). Mobile laser scanning in fluvial geomorphology: Mapping and change detection of point bars. *Zeitschrift Für Geomorphologie, Supplementary Issues*, *55*(2), 31–50. https://doi.org/10.1127/0372-8854/2011/0055S2-0044

Alioravainen, N., Orell, P., & Erkinaro, J. (2023). Long-Term Trends in Freshwater and Marine Growth Patterns in Three Sub-Arctic Atlantic Salmon Populations. *Fishes*, *8*(9), Article 9. https://doi.org/10.3390/fishes8090441

Amad, P. (2012). From God's-eye to Camera-eye: Aerial Photography's Post-humanist and Neo-humanist Visions of the World. *History of Photography*, *36*(1), 66–86. https://doi.org/10.1080/03087298.2012.632567

Arbogast, A. F. (2017). *Discovering physical geography* (Fourth edition.). John Wiley & Sons.

Bennett, K. E., Miller, G., Busey, R., Chen, M., Lathrop, E. R., Dann, J. B., Nutt, M., Crumley, R., Dillard, S. L., Dafflon, B., Kumar, J., Bolton, W. R., Wilson, C. J., Iversen, C. M., & Wullschleger, S. D. (2022). Spatial patterns of snow distribution in the sub-Arctic. *The Cryosphere*, *16*(8), 3269–3293. https://doi.org/10.5194/tc-16-3269-2022

Beven, K. J., & Kirkby, M. J. (1979). A physically based, variable contributing area model of basin hydrology. *Hydrological Sciences Bulletin*, *24*(1), 43–69. https://doi.org/10.1080/02626667909491834

Bowker, D. E., Davis, R. E., Myrick, D. L., Stacy, K., & Jones, W. T. (1985). *Spectral reflectances of natural targets for use in remote sensing studies* (Vol. 1139). NASA.

Bukata, R. P., Jerome, J. H., Kondratyev, A. S., & Pozdnyakov, D. V. (1995). *Optical Properties and Remote Sensing of Inland and Coastal Waters*. CRC Press.

Campbell, J. B., Thomas, V. A., & Wynne, R. H. (2022). *Introduction to remote sensing* (Sixth edition.). Guilford Publications.

Carrara, A., Cardinali, M., Detti, R., Guzzetti, F., Pasqui, V., & Reichenbach, P. (1991). GIS techniques and statistical models in evaluating landslide hazard. *Earth Surface Processes and Landforms*, *16*(5), 427–445. https://doi.org/10.1002/esp.3290160505

Collinson, J. D. (1970). Bedforms of the Tana River, Norway. *Geografiska Annaler: Series A, Physical Geography*, *52*(1), 31–56. https://doi.org/10.1080/04353676.1970.11879807

Curran, P. J., & Novo, E. M. M. (1988). The Relationship Between Suspended Sediment Concentration and Remotely Sensed Spectral Radiance: A Review. *Journal of Coastal Research*, *4*(3), 351–368.

Dahlke, H. E., Lyon, S. W., Stedinger, J. R., Rosqvist, G., & Jansson, P. (2012). Contrasting trends in floods for two sub-arctic catchments in northern Sweden – does glacier presence matter? *Hydrology and Earth System Sciences*, *16*(7), 2123–2141. https://doi.org/10.5194/hess-16-2123-2012

Djokic, D., & Maidment, D. R. (1991). Terrain analysis for urban stormwater modelling. *Hydrological Processes*, *5*(1), 115–124. https://doi.org/10.1002/hyp.3360050109

Duggin, M. J. (1985). Review Article Factors limiting the discrimination and quantification of terrestrial features using remotely sensed radiance. *International Journal of Remote Sensing*, *6*(1), 3–27. https://doi.org/10.1080/01431168508948420

Eilertsen, R., & Corner, G. (2011). *Role of Scouring and Base-Level Change in Producing Anomalously Thick Fluvial Successions: An Example from the Tana River, Northern Norway* (pp. 265–279). https://doi.org/10.2110/sepmsp.097.265

El Mahrad, B., Newton, A., Icely, J. D., Kacimi, I., Abalansa, S., & Snoussi, M. (2020). Contribution of Remote Sensing Technologies to a Holistic Coastal and Marine Environmental Management Framework: A Review. *Remote Sensing*, *12*(14), Article 14. https://doi.org/10.3390/rs12142313

Elmore, P., & Steed, C. (2008). *Algorithm Design Study for Bathymetry Fusion—Review of Current State-of-the-art and Recommended Design Approach* (NRL/FR/7440--08-10,162).

ESA. (n.d.). *User Guides—Sentinel-2 MSI - Revisit and Coverage—Sentinel Online*. Sentinel Online. Retrieved April 6, 2023, from https://copernicus.eu/user-guides/sentinel-2-msi/revisit-coverage

Evagorou, E., Argyriou, A., Papadopoulos, N., Mettas, C., Alexandrakis, G., & Hadjimitsis, D. (2022). Evaluation of Satellite-Derived Bathymetry from High and Medium-Resolution Sensors Using Empirical Methods. *Remote Sensing*, *14*(3), 772. https://doi.org/10.3390/rs14030772

Fitzpatrick, A., Singhvi, A., & Arbabian, A. (2020). An Airborne Sonar System for Underwater Remote Sensing and Imaging. *IEEE Access*, *8*, 189945–189959. https://doi.org/10.1109/ACCESS.2020.3031808

Flener, C. (2013). Estimating deep water radiance in shallow water: Adapting optical bathymetry modelling to shallow river environments. *Boreal Environment Research*, *18*, 488–502.

Flener, C., Lotsari, E., Alho, P., & Käyhkö, J. (2012). Comparison of empirical and theoretical remote sensing based bathymetry models in river environments. *River Research and Applications*, *28*(1), 118–133. https://doi.org/10.1002/rra.1441

Ford, J., & Bedford, B. L. (1987). The Hydrology of Alaskan Wetlands, U.S.A.: A Review. *Arctic and Alpine Research*, *19*(3), 209–229. https://doi.org/10.1080/00040851.1987.12002596

Fossøy, F., Erkinaro, J., Orell, P., Pohjola, J.-P., Brandsegg, H., Andersskog, I. P. Ø., & Sivertsgård, R. (2022). Monitoring the pink salmon invasion in Tana using eDNA. Assessment of pink salmon, Atlantic salmon and European bullhead. In *23*. Norwegian Institute for Nature Research (NINA). https://brage.nina.no/nina-xmlui/handle/11250/3036089

Gao, J. (2009). Bathymetric mapping by means of remote sensing: Methods, accuracy and limitations. *Progress in Physical Geography: Earth and Environment*, *33*(1), 103–116. https://doi.org/10.1177/0309133309105657

Gessler, P. E., Moore, I. D., McKenzie, N. J., & Ryan, P. J. (1995). Soil-landscape modelling and spatial prediction of soil attributes. *International Journal of Geographical Information Systems*, *9*(4), 421–432. https://doi.org/10.1080/02693799508902047

Goetz, A. F. H., Rock, B. N., & Rowan, L. C. (1983). Remote sensing for exploration; an overview. *Economic Geology*, *78*(4), 573–590. https://doi.org/10.2113/gsecongeo.78.4.573

Gould, W. A., & Walker, M. D. (1999). Plant communities and landscape diversity along a Canadian Arctic river. *Journal of Vegetation Science*, *10*(4), 537–548. https://doi.org/10.2307/3237188

Guenther, G., Cunningham, A., Laroque, P., & Reid, D. (2000). Meeting the Accuracy Challenge in Airborne Bathymetry. *Proceedings of the 20th EARSeL Symposium*. https://apps.dtic.mil/sti/citations/ADA488934

Hare, F. K. (1951). Some Climatological Problems of the Arctic and Sub-Arctic. In H. R. Byers, H. E. Landsberg, H. Wexler, B. Haurwitz, A. F. Spilhaus, H. C. Willett, H. G. Houghton, & T. F. Malone (Eds.), *Compendium of Meteorology: Prepared under the Direction of the Committee on the Compendium of Meteorology* (pp. 952–964). American Meteorological Society. https://doi.org/10.1007/978-1-940033-70-9_76

Huang, J., Zhang, X., Zhang, Q., Lin, Y., Hao, M., Luo, Y., Zhao, Z., Yao, Y., Chen, X., Wang, L., Nie, S., Yin, Y., Xu, Y., & Zhang, J. (2017). Recently amplified arctic warming has contributed to a continual global warming trend. *Nature Climate Change*, *7*(12), Article 12. https://doi.org/10.1038/s41558-017-0009-5

Hutchinson, M. F., & Dowling, T. I. (1991). A continental hydrological assessment of a new grid-based digital elevation model of Australia. *Hydrological Processes*, *5*(1), 45–58. https://doi.org/10.1002/hyp.3360050105

Isaacs, R. G., Hoffman, R. N., & Kaplan, L. D. (1986). Satellite remote sensing of meteorological parameters for global numerical weather prediction. *Reviews of Geophysics*, *24*(4), 701–743. https://doi.org/10.1029/RG024i004p00701

Janowski, L., Wroblewski, R., Dworniczak, J., Kolakowski, M., Rogowska, K., Wojcik, M., & Gajewski, J. (2021). Offshore benthic habitat mapping based on object-based image analysis and geomorphometric approach. A case study from the Slupsk Bank, Southern Baltic Sea. *Science of The Total Environment*, *801*, 149712. https://doi.org/10.1016/j.scitotenv.2021.149712

Jawak, S. D., Vadlamani, S. S., & Luis, A. J. (2015). A Synoptic Review on Deriving Bathymetry Information Using Remote Sensing Technologies: Models, Methods and Comparisons. *Advances in Remote Sensing*, *04*(02), Article 02. https://doi.org/10.4236/ars.2015.42013

Johnson, W. D. (1887). The Term "Topography." *Science*, *10*(242), 152–153. https://doi.org/10.1126/science.ns-10.242.152.c

Jupp, D. L. B., Mayo, K. K., Kuchler, D. A., Claasen, D. V. R., Kenchington, R. A., & Guerin, P. R. (1985). Remote sensing for planning and managing the great barrier reef of Australia. *Photogrammetria*, *40*(1), 21–42. https://doi.org/10.1016/0031-8663(85)90043-2

Kairu, E. N. (1982). An Introduction to Remote Sensing. *GeoJournal*, *6*(3), 251–260.

Kasvi, E., Salmela, J., Lotsari, E., Kumpula, T., & Lane, S. N. (2019). Comparison of remote sensing based approaches for mapping bathymetry of shallow, clear water rivers. *Geomorphology*, *333*, 180–197. https://doi.org/10.1016/j.geomorph.2019.02.017

Kinzel, P. J., Legleiter, C. J., & Nelson, J. M. (2013). Mapping River Bathymetry With a Small Footprint Green LiDAR: Applications and Challenges1. *JAWRA Journal of the American Water Resources Association*, *49*(1), 183–204. https://doi.org/10.1111/jawr.12008

Kinzel, P. J., Wright, C. W., Nelson, J. M., & Burman, A. R. (2007). Evaluation of an Experimental LiDAR for Surveying a Shallow, Braided, Sand-Bedded River. *USGS Staff -- Published Research*. https://digitalcommons.unl.edu/usgsstaffpub/77

Kogut, P. (2020, November 18). Types Of Remote Sensing: Devices And Their Applications. *EOSDA Blog*. https://eos.com/blog/types-of-remote-sensing/

Lax, H. G., Koskenniemi, E., Sevola, P., & Bagge, P. (1993). Tenojoen pohjaeläimistö ympärstön laadun kuvaajana. *Vesi- ja ympäristöhallitus*, *Vesi-ja ympäristöhallinnon julkaisuja, sarja A*(131), 124.

Legleiter, C. J. (2012). Remote measurement of river morphology via fusion of LiDAR topography and spectrally based bathymetry. *Earth Surface Processes and Landforms*, *37*(5), 499–518. https://doi.org/10.1002/esp.2262

Legleiter, C. J., & Roberts, D. A. (2005). Effects of channel morphology and sensor spatial resolution on image-derived depth estimates. *Remote Sensing of Environment*, *95*(2), 231–247. https://doi.org/10.1016/j.rse.2004.12.013

Li, J., Knapp, D. E., Lyons, M., Roelfsema, C., Phinn, S., Schill, S. R., & Asner, G. P. (2021). Automated Global Shallow Water Bathymetry Mapping Using Google Earth Engine. *Remote Sensing*, *13*(8), Article 8. https://doi.org/10.3390/rs13081469

Lintz, J., & Simonett, D. S. (1976). Sensors for spacecraft. In *Remote Sensing of Environment* (pp. 323–343). https://ui.adsabs.harvard.edu/abs/1976rse..book..323L

Lotsari, E. (2023, October 27). *Changing cold climate river environments*. The Geographical Society of Finland Palmén colloquium, Zoom.

Lotsari, E., Hackney, C., Salmela, J., Kasvi, E., Kemp, J., Alho, P., & Darby, S. e. (2020). Sub-arctic river bank dynamics and driving processes during the open-channel flow period. *Earth Surface Processes and Landforms*, *45*(5), 1198–1216. https://doi.org/10.1002/esp.4796

Lotsari, E., Lintunen, K., Kasvi, E., Alho, P., & Blåfield, L. (2022). The impacts of near-bed flow characteristics on river bed sediment transport under ice-covered conditions in 2016–2021. *Journal of Hydrology*, *615*, 128610. https://doi.org/10.1016/j.jhydrol.2022.128610

Lotsari, E., Veijalainen, N., Alho, P., & Käyhkö, J. (2010). Impact of climate change on future discharges and flow characteristics of the tana river, sub-arctic northern fennoscandia. *Geografiska Annaler: Series A, Physical Geography*, *92*(2), 263–284. https://doi.org/10.1111/j.1468-0459.2010.00394.x

Lotsari, E., Wang, Y., Kaartinen, H., Jaakkola, A., Kukko, A., Vaaja, M., Hyyppä, H., Hyyppä, J., & Alho, P. (2015). Gravel transport by ice in a subarctic river from accurate laser scanning. *Geomorphology*, *246*, 113–122. https://doi.org/10.1016/j.geomorph.2015.06.009

Lyzenga, D. R. (1978). Passive remote sensing techniques for mapping water depth and bottom features. *Applied Optics*, *17*(3), 379. https://doi.org/10.1364/AO.17.000379

Magnuson, J. J., Robertson, D. M., Benson, B. J., Wynne, Randolph H., Livingstone, D. M., Arai, T., Assel, R. A., Barry, R. G., Card, V., Kuusisto, E., Granin, N. G., Prowse, T. D., Stewart, K. M., & Vuglinski, V. S. (2000). Historical Trends in Lake and River Ice Cover in the Northern Hemisphere. *Science*, *289*(5485), 1743–1746. https://doi.org/10.1126/SCIENCE.289.5485.1743

Mahiny, A. S., & Turner, B. J. (2007). A Comparison of Four Common Atmospheric Correction Methods. *Photogrammetric Engineering & Remote Sensing*, *73*(4), 361–368. https://doi.org/10.14358/PERS.73.4.361

Mandlburger, G., Pfennigbauer, M., & Pfeifer, N. (2013). Analyzing near water surface penetration in laser bathymetry – A case study at the River Pielach. *ISPRS Annals of the Photogrammetry, Remote Sensing and Spatial Information Sciences*, *II-5/W2*, 175–180. https://doi.org/10.5194/isprsannals-II-5-W2-175-2013

Mansikkaniemi, H. (1970). Deposits of sorted material in the Inarijoki-Tana river valley in Lapland. *Annales Universitatis Turkuensis*, *A II*(43).

Miller, R. L., & McKee, B. A. (2004). Using MODIS Terra 250 m imagery to map concentrations of total suspended matter in coastal waters. *Remote Sensing of Environment*, *93*(1), 259–266. https://doi.org/10.1016/j.rse.2004.07.012

Milne, J. A., & Sear, D. A. (1997). Modelling river channel topography using GIS. *International Journal of Geographical Information Science*, *11*(5), 499–519. https://doi.org/10.1080/136588197242275

Nironen, M. (2017). Guide to the Geological Map of Finland – Bedrock 1:1 000 000. *Geological Survey of Finland, Special Paper*, *60*, 41–76.

NOAA. (n.d.). *What is bathymetry?* Retrieved April 6, 2023, from https://oceanservice.noaa.gov/facts/bathymetry.html

Nylén, T., Kasvi, E., Salmela, J., Kaartinen, H., Kukko, A., Jaakkola, A., Hyyppä, J., & Alho, P. (2019). Improving distribution models of riparian vegetation with mobile laser scanning and hydraulic modelling. *PLOS ONE*, *14*(12), e0225936. https://doi.org/10.1371/journal.pone.0225936

Orange, D. L., Teas, P. A., Decker, J., & Gharib, J. (2022). Use of multibeam bathymetry and backscatter to improve seabed geochemical surveys: Part 1, historical review, technical description, and best practices. *Interpretation*, 1–132. https://doi.org/10.1190/int-2021-0236.1

Panhalkar, S. S., & Jarag, A. P. (2015). Assessment of Spatial Interpolation Techniques for River Bathymetry Generation of Panchganga River Basin Using Geoinformatic Techniques. *Asian Journal of Geoinformatics*, *15*(3), 9–15.

Pettorelli, N., Laurance, W. F., O'Brien, T. G., Wegmann, M., Nagendra, H., & Turner, W. (2014). Satellite remote sensing for applied ecologists: Opportunities and challenges. *Journal of Applied Ecology*, *51*(4), 839–848. https://doi.org/10.1111/1365-2664.12261

Planck, M. (1901). On the Law of Distribution of Energy in the Normal Spectrum. *Annalen Der Physik*, *4*(553). http://dbhs.wvusd.k12.ca.us/webdocs/Chem-History/Planck-1901/Planck-1901.html

Quinn, P., Beven, K., Chevallier, P., & Planchon, O. (1991). The prediction of hillslope flow paths for distributed hydrological modelling using digital terrain models. *Hydrological Processes*, *5*(1), 59–79. https://doi.org/10.1002/hyp.3360050106

Rantanen, M., Karpechko, A. Y., Lipponen, A., Nordling, K., Hyvärinen, O., Ruosteenoja, K., Vihma, T., & Laaksonen, A. (2022). The Arctic has warmed nearly four times faster than the globe since 1979. *Communications Earth & Environment*, *3*(1), Article 1. https://doi.org/10.1038/s43247-022-00498-3

Ritchie, J. C., Schiebe, F. R., & McHenry, J. R. (1976). Remote Sensing of Suspended Sediments in Surface Waters. *Photogrammetric Engineering & Remote Sensing*, *42*(12), 1539–1545.

Ritchie, J. C., Zimba, P. V., & Everitt, J. H. (2003). Remote Sensing Techniques to Assess Water Quality. *Photogrammetric Engineering & Remote Sensing*, *69*(6), 695–704. https://doi.org/10.14358/PERS.69.6.695

Ruppel, M. M., Eckhardt, S., Pesonen, A., Mizohata, K., Oinonen, M. J., Stohl, A., Andersson, A., Jones, V., Manninen, S., & Gustafsson, Ö. (2021). Observed and Modeled Black Carbon Deposition and Sources in the Western Russian Arctic 1800–2014. *Environmental Science & Technology*, *55*(8), 4368–4377. https://doi.org/10.1021/acs.est.0c07656

Said, M. N., Mahmud, M. R., & Hasan, R. C. (2018). Evaluating satellite-derived bathymetry accuracy from Sentinel-2A high-resolution multispectral imageries for shallow water hydrographic mapping. *IOP Conference Series: Earth and Environmental Science*, *169*, 012069. https://doi.org/10.1088/1755-1315/169/1/012069

Schimel, A. C. G., Beaudoin, J., Parnum, I. M., Le Bas, T., Schmidt, V., Keith, G., & Ierodiaconou, D. (2018). Multibeam sonar backscatter data processing. *Marine Geophysical Research*, *39*(1–2), 121–137. https://doi.org/10.1007/s11001-018-9341-z

Schwabe, J., Ågren, J., Liebsch, G., Westfeld, P., Hammarklint, T., Mononen, J., & Andersen, O. B. (2020). The Baltic Sea Chart Datum 2000 (BSCD2000): Implementation of a common reference level in the Baltic Sea. *The International Hydrographic Review*, *23*, Article 23.

Shintani, C., & Fonstad, M. A. (2017). Comparing remote-sensing techniques collecting bathymetric data from a gravel-bed river. *International Journal of Remote Sensing*, *38*(8–10), 2883–2902. https://doi.org/10.1080/01431161.2017.1280636

Šiljeg, A., Lozić, S., & Šiljeg, S. (2015). A comparison of interpolation methods on the basis of data obtained from a bathymetric survey of Lake Vrana, Croatia. *Hydrology and*

Earth System Sciences, *19*(8), 3653–3666. https://doi.org/10.5194/hess-19-3653-2015

Smeed, D. A., Josey, S. A., Beaulieu, C., Johns, W. E., Moat, B. I., Frajka-Williams, E., Rayner, D., Meinen, C. S., Baringer, M. O., Bryden, H. L., & McCarthy, G. D. (2018). The North Atlantic Ocean Is in a State of Reduced Overturning. *Geophysical Research Letters*, *45*(3), 1527–1533. https://doi.org/10.1002/2017GL076350

Song, Y., & Wu, P. (2021). Earth Observation for Sustainable Infrastructure: A Review. *Remote Sensing*, *13*(8), Article 8. https://doi.org/10.3390/rs13081528

Tribe, A. (1992). Automated recognition of valley lines and drainage networks from grid digital elevation models: A review and a new method. *Journal of Hydrology*, *139*(1), 263–293. https://doi.org/10.1016/0022-1694(92)90206-B

Turcotte, B., Morse, B., Bergeron, N. E., & Roy, A. G. (2011). Sediment transport in ice-affected rivers. *Journal of Hydrology*, *409*(1), 561–577. https://doi.org/10.1016/j.jhydrol.2011.08.009

Vachon, D., Sponseller, R. A., & Karlsson, J. (2021). Integrating carbon emission, accumulation and transport in inland waters to understand their role in the global carbon cycle. *Global Change Biology*, *27*(4), 719–727. https://doi.org/10.1111/gcb.15448

Vieux, B. E. (1991). Geographic information systems and non-point source water quality and quantity modelling. *Hydrological Processes*, *5*(1), 101–113. https://doi.org/10.1002/hyp.3360050108

Weyhenmeyer, G. A., Livingstone, D. M., Meili, M., Jensen, O., Benson, B., & Magnuson, J. J. (2011). Large geographical differences in the sensitivity of ice-covered lakes and rivers in the Northern Hemisphere to temperature changes. *Global Change Biology*, *17*(1), 268–275. https://doi.org/10.1111/j.1365-2486.2010.02249.x

Wölfl, A.-C., Snaith, H., Amirebrahimi, S., Devey, C. W., Dorschel, B., Ferrini, V., Huvenne, V. A. I., Jakobsson, M., Jencks, J., Johnston, G., Lamarche, G., Mayer, L., Millar, D., Pedersen, T. H., Picard, K., Reitz, A., Schmitt, T., Visbeck, M., Weatherall, P., &

Wigley, R. (2019). Seafloor Mapping – The Challenge of a Truly Global Ocean Bathymetry. *Frontiers in Marine Science*, *6*. https://www.frontiersin.org/articles/10.3389/fmars.2019.00283

Woodget, A. S., Carbonneau, P. E., Visser, F., & Maddock, I. P. (2015). Quantifying submerged fluvial topography using hyperspatial resolution UAS imagery and structure from motion photogrammetry. *Earth Surface Processes and Landforms*, *40*(1), 47–64. https://doi.org/10.1002/esp.3613

Wright, A. C., & Webster, R. (1991). A stochastic distributed model of soil erosion by overland flow. *Earth Surface Processes and Landforms*, *16*(3), 207–226. https://doi.org/10.1002/esp.3290160303

Zhao, Q., Yu, L., Du, Z., Peng, D., Hao, P., Zhang, Y., & Gong, P. (2022). An Overview of the Applications of Earth Observation Satellite Data: Impacts and Future Trends. *Remote Sensing*, *14*(8), Article 8. https://doi.org/10.3390/rs14081863

Zheng, S., Cheng, H., Tang, M., Xu, W., Liu, E., Gao, S., Best, J., Jiang, Y., & Zhou, Q. (2022). Sand mining impact on Poyang Lake: A case study based on high-resolution bathymetry and sub-bottom data. *Journal of Oceanology and Limnology*, *40*(4), 1404–1416. https://doi.org/10.1007/s00343-021-1137-3

Zhou, Y., Lu, L., Li, L., Zhang, Q., & Zhang, P. (2021). A Generic Method to Derive Coastal Bathymetry From Satellite Photogrammetry for Tsunami Hazard Assessment. *Geophysical Research Letters*, *48*(21), e2021GL095142. https://doi.org/10.1029/2021GL095142

Appendices

The main heading of the appendices is not numbered. The same styles are used in the appendices as in the text chapters.

Appendix 1 Heading

Each appendix is numbered and given a heading.

Appendix 2 Heading

You can start each appendix from a new page if you wish.